

RESEARCH ARTICLE

Functional genomics of trypanotolerant and trypanosusceptible cattle infected with *Trypanosoma congolense* across multiple time points and tissues

Gillian P. McHugo¹, James A. Ward¹, John A. Browne¹, Grace M. O’Gorman², Kieran G. Meade^{1,3}, Emmeline W. Hill¹, Thomas J. Hall¹, David E. MacHugh^{1,3,4*}

1 UCD School of Agriculture and Food Science, University College Dublin, Belfield, Dublin, Ireland, **2** UK Agri-Tech Centre, Innovation Centre, York Science Park, York, United Kingdom, **3** UCD Conway Institute of Biomolecular and Biomedical Research, University College Dublin, Dublin, Ireland, **4** UCD One Health Centre, University College Dublin, Dublin, Ireland

* david.machugh@ucd.ie



OPEN ACCESS

Citation: McHugo GP, Ward JA, Browne JA, O’Gorman GM, Meade KG, Hill EW, et al. (2025) Functional genomics of trypanotolerant and trypanosusceptible cattle infected with *Trypanosoma congolense* across multiple time points and tissues. PLoS Negl Trop Dis 19(8): e0012882. <https://doi.org/10.1371/journal.pntd.0012882>

Editor: Nilson I.T. Zanchin, Oswaldo Cruz Foundation: Fundacao Oswaldo Cruz, BRAZIL

Received: January 30, 2025

Accepted: July 6, 2025

Published: August 4, 2025

Copyright: © 2025 McHugo et al. This is an open access article distributed under the terms of the [Creative Commons Attribution License](#), which permits unrestricted use, distribution, and reproduction in any medium, provided the original author and source are credited.

Data availability statement: Affymetrix GeneChip Bovine Genome Array data sets generated for this study have been deposited in the European Molecular Biology Laboratory European Bioinformatics Institute ArrayExpress

Abstract

Human African trypanosomiasis (HAT), or sleeping sickness, is a neglected tropical disease caused by infection with trypanosome parasites (*Trypanosoma* spp.). These are transmitted by infected tsetse flies (*Glossina* spp.) and cause a similar disease in animals, known as African animal trypanosomosis (AAT), which is one of the largest constraints to livestock production in sub-Saharan Africa and causes a financial burden of approximately \$4.5 billion annually. Some African *Bos taurus* cattle populations have an important evolutionary adaptation known as trypanotolerance, a genetically determined tolerance of infection by trypanosome parasites (*Trypanosoma* spp.). Trypanotolerant African *B. taurus* N’Dama and trypanosusceptible *Bos indicus* Boran cattle responded in largely similar ways during trypanosome infection when gene expression was examined using blood, liver, lymph node, and spleen samples with peaks and troughs of gene expression differences following the cyclic pattern of parasitaemia exhibited during trypanosome infection. However, differences in response to infection between the two breeds were reflected in differential expression of genes related to the immune system such as those encoding antimicrobial peptides and cytokines, including, for example, the antimicrobial peptide encoding genes *LEAP2*, *CATHL3*, *DEFB4A*, and *S100A7* and the cytokine genes *CCL20*, *CXCL11*, *CXCL13*, *CXCL16*, *CXCL17*, *IL33*, and *TNFSF13B*. In addition, transcriptional profiling of peripheral blood identified expression differences in genes relating to coagulation and iron homeostasis, which supports the hypothesis that the dual control of parasitaemia and the anaemia resulting from the innate immune response to trypanosome parasites is key to trypanotolerance and provide new insights into the molecular mechanisms underlying this phenomenon.

data repository (www.ebi.ac.uk/biostudies/arrayexpress) under accession number E-MTAB-14517.

Funding: This research work was funded by Science Foundation Ireland (SFI; sfi.ie) under Investigator Programme Awards to D.E.M. (grant nos: SFI/01/F.1/B028 and SFI/15/IA/3154). J.A.W. was supported by the SFI Centre for Research Training in Genomics Data Science (grant no. 18/CRT/6214). Note: Science Foundation Ireland is now Research Ireland (www.researchireland.ie). The funder did not play any role in the study design, data collection and analysis, decision to publish, or preparation of the manuscript

Competing interests: The authors have declared that no competing interests exist.

Author summary

Trypanosome parasites are transmitted by infected tsetse flies and cause the neglected tropical disease human African trypanosomiasis (HAT) and the similar African animal trypanosomosis (AAT), which is one of the largest impediments to livestock production in sub-Saharan Africa. Taurine (*Bos taurus*) and indicine (*Bos indicus*) cattle shared a common ancestor more than 150,000 years ago, and in the intervening period significant genomic differences have evolved between the two groups. Importantly, several African *B. taurus* populations have evolved an adaptation known as trypanotolerance, a genetically determined tolerance of infection by trypanosome parasites. Trypanotolerant African taurine and trypanosusceptible indicine cattle responded in largely similar ways during trypanosome infection when gene expression was examined using blood, liver, lymph node, and spleen samples with peaks and troughs of gene expression differences following the cyclic pattern of the number of trypanosome parasites in the blood. Transcriptional profiling of these tissues highlighted genes related to the multiple facets of the immune system; notably, for peripheral blood, differences observed for genes relating to coagulation and iron homeostasis support the existing hypothesis that control of both parasite number and anaemia is an important feature of the trypanotolerance trait and provide new insights into the molecular mechanisms underlying this phenomenon.

Introduction

Trypanosomiasis is prevalent in humid and semi-humid regions of Africa and is a wasting disease caused by parasitic protozoa of the genus *Trypanosoma* which are transmitted by biting insect vectors such as tsetse flies (*Glossina* spp.) [1]. Human African trypanosomiasis (HAT), caused by *T. brucei gambiense* or *T. brucei rhodesiense* infection, is also known as sleeping sickness and is classed as a neglected tropical disease (NTD) by the World Health Organisation [2]. Trypanosomes also infect animals and cause particularly severe disease in domesticated animals—African animal trypanosomosis (AAT)—for which the symptoms, as in HAT, include fever, severe weight loss, and anaemia [1,3,4]. As the disease progresses, animals weaken and become paralysed and unfit for work [1]. AAT is caused by a wider range of trypanosome parasites, most commonly *T. congolense*, *T. vivax*, and *T. brucei* ssp., although the prevalence and distribution of trypanosome species varies and co-infections are possible [5,6]. In addition, domestic animals can also be infected with the human-infective trypanosome species, for which they act as a reservoir [5,7]. Due to the importance of livestock to human livelihoods, and therefore human health, there have also been calls to class AAT as a NTD in its own right [8].

Animal models, including mice, have long been used to study human-infective trypanosomes leading to important insights into host-trypanosome interactions [9–11]. The usefulness of these animal models has been improved by the differential

host tolerance of, or susceptibility to, trypanosome infection that has been found between different cattle breeds, mouse strains, and human populations, although the underlying genes differ between host species [12–15]. Conversely, while it is much less common, humans may also be infected with trypanosome species more frequently found in animals, resulting in atypical human trypanosomiasis [5,16]. With climate change and increasing globalisation there is growing concern that this atypical human trypanosomiasis may represent an emerging neglected zoonotic disease that underscores the importance of a One Health approach to both human and animal trypanosomiasis [17]. Trypanosomiasis has a limiting effect on sub-Saharan livestock production, because even with application of trypanocidal drugs, the susceptibility of most cattle to trypanosomiasis makes production economically unsustainable in many regions on the African continent [18].

Cattle are significant components of rural economies and livelihoods in Africa. They provide milk, meat, fertiliser and traction and represent mobile assets that serve as a financial buffer for poor families, particularly for pastoralists and women [19,20]. There are approximately 150 breeds of indigenous cattle in sub-Saharan Africa and African cattle represent a complex mosaic of African *Bos taurus*, European *B. taurus*, *B. indicus*, and various hybrid populations [21–23]. African cattle form a gradient of *B. taurus* and *B. indicus* ancestry across the continent [21]. This is a result of multiple domestications and the subsequent spread of distinct populations of cattle across Africa [24]. The spread of agriculture and livestock herding has also shaped African human genetics and linguistic variation, illustrating the importance of domesticated species in influencing recent human evolution [25,26]. Zebu or indicine breeds, which have primarily *B. indicus* ancestry, are favoured by many farmers due to their larger size and higher production yields [27]. However, cattle populations in West Africa tend to have higher level of taurine (*B. taurus*) ancestry [21,28]. This is because some indigenous *B. taurus* breeds have an advantage in western sub-Saharan Africa due to their tolerance of trypanosomes, a trait termed “trypanotolerance” [27,29]. These cattle exhibit a greater ability to control parasitaemia and anaemia, making them more productive than *B. indicus* cattle or other *B. taurus* breeds in areas infested with tsetse flies and trypanosomes [27,30]. These trypanotolerant breeds, which include the longhorn N'Dama and shorthorn Baoule, Lagune, and Somba breeds, are therefore an important genetic resource as they are uniquely suited to livestock production in these areas [31,32]. Trypanotolerant breeds only make up 6% of the total cattle population of Africa and but represent 17% of the cattle in the tsetse infested areas [33]. Although trypanotolerance is a valuable trait in these areas, trypanotolerant breeds such as the N'Dama, are not more widely used because of their relatively inferior production characteristics, unpredictable temperament and smaller size, which make them unsuitable for draft purposes [33,34].

Trypanotolerance has been shown to be a heritable trait, although there is variability in tolerance between animals within breeds [14,30,35,36]. Trypanotolerant breeds are also less susceptible to other infectious diseases such as helminthiasis, ticks and tick-borne-diseases and genes associated with the immune response have been found to be under selection in west African cattle populations [37,38]. Trypanotolerant and trypanosusceptible breeds have been shown to vary in their immune responses and exhibit gene expression differences in various tissues at key points during infection after infection with trypanosomes [34,39–43]. They also show differences in ability to control anaemia over two years [44]. There are also *B. taurus/B. indicus* hybrid breeds that have been observed to be trypanotolerant [45]. However, trypanotolerant breeds with high levels of African *B. taurus* ancestry are better able to control anaemia while hybrid animals exhibit intermediate levels of control when compared to susceptible *B. indicus* breeds [46]. The genes, genomic regulatory elements (GREGs), and genomic regulatory networks (GRNs) underpinning trypanotolerance remain largely unknown, although several candidate genes and regulatory mechanisms have been suggested based on population genomics and functional genomics studies [34,41,43,44,47–50]. It has been proposed that a better understanding of the trypanotolerance trait will facilitate genome-informed breeding programmes that could also leverage transgenesis to enhance the trait, thereby increasing the productivity of livestock production in sub-Saharan Africa [27,34].

In this study we analysed Affymetrix Bovine Genome Array gene expression data across multiple tissues from trypanotolerant N'Dama and trypanosusceptible Boran cattle that had been infected with *T. congolense* across an infection time course [34,41,42]. We used previously published data from liver, lymph node, and spleen tissue samples and combined

these data with new peripheral blood mononuclear cell (PBMC) data from the same animals. Differentially expressed genes (DEGs) were detected across the infection time course for each breed and between the two breeds for each time point. The sets of DEGs were then used for functional enrichment analyses focused on gene ontology (GO) to catalogue and interrogate biological processes associated with disease pathogenesis and trypanotolerance.

Materials and methods

Data sources

Ethics statement. This animal work was completed prior to the requirement for formal Institutional Permission in Ireland, which is based on European Union Directive 2010/63/EU; however, all animal procedures were approved by the Institutional Animal Use and Care (IAUC) Committee of ILRI in accordance with the UK Animals (Scientific Procedures) Act 1986 and all efforts were made to ensure high welfare standards and ethical handling of animal subjects.

New microarray gene expression data. Affymetrix Bovine Genome Array data sets were generated for 40 peripheral blood mononuclear cell (PBMC) samples from 10 African cattle (5 trypanotolerant N'Dama and 5 trypanosusceptible Boran) collected at four time points for a *T. congolense* infection experiment performed in 2003 [40–42]. The cattle, all female and aged between 19–28 months, were reared together at the International Livestock Research Institute (ILRI) ranch at Kapiti Plains Estate, Kenya which is located in an area free from tsetse flies and trypanosomiasis [42]. The cattle were experimentally infected with the *T. congolense* clone IL1180 [51,52] delivered via the bites of eight infected tsetse flies (*Glossina morsitans morsitans*) [53,54] at the ILRI laboratories in Nairobi, Kenya. The flies were allowed to feed on the shaved flanks of the animals until engorgement. The infections were carried out in three batches which took place two weeks apart and were confirmed by microscopy. Parasitaemia and anaemia measured by packed cell volume (PCV) were monitored throughout the course of the infection [42]. Peripheral blood (200 ml) was collected in heparinised syringes before infection and at 14, 25, and 34 days post-infection (dpi), these time points were selected to align with the first wave of parasitaemia [42]. Peripheral blood mononuclear cell (PBMC) samples were isolated from the blood samples with Percoll gradients (GE Healthcare, Buckinghamshire, UK) and total RNA was extracted from the PBMCs in TriReagent (Molecular Research Center, Inc., Cincinnati, OH, USA) and the RNA samples were then DNase-treated and purified using an RNeasy mini kit (Qiagen Ltd., Crawley, UK). RNA quality and quantity was assessed using the 18S/28S ratio and RNA integrity number (RIN) on an Agilent Bioanalyzer with the RNA 6000 Nano LabChip kit (Agilent Technologies, Inc., Santa Clara, CA, USA). Following this, cDNA labelling, hybridisation and scanning for the microarray experiments were performed by Almac Diagnostic Services (Craigavon, Northern Ireland) using a one-cycle amplification/labelling protocol. Gene expression data in the form of cell intensity files (.CEL) were generated using the Affymetrix GeneChip Operating Software (GCOS) package. The Affymetrix GeneChip Bovine Genome Array data sets generated for this study have been deposited in the European Molecular Biology Laboratory European Bioinformatics Institute ArrayExpress data repository under accession number E-MTAB-14517.

Previously published microarray gene expression data. Additional Affymetrix Bovine Genome Array data sets were obtained from a published study using solid tissues samples from the same animal infection time course [34] resulting in a total of 220 biological samples across 12 infection time points and four tissues (for both N'Dama and Boran) before filtering (Table 1). Fig 1 illustrates the experimental design and study workflow. The computer code required to repeat and reproduce the analyses is available at [www.doi.org/10.5281/zenodo.11502109](https://doi.org/10.5281/zenodo.11502109).

Data filtering and normalisation

Quality control with log transformation was performed using affy (v. 1.80.0) [57], Biobase (v. 2.62.0) [58], and arrayQualityMetrics (v. 3.58.0) [59] with R (v. 4.3.2) [60]. As in previous microarray studies, any individual samples that were identified as outliers in two or more quality control tests were discarded from the analysis [61]. Normalisation was performed using farms (v. 1.25.0) [62] with R (v. 4.3.2).

Table 1. Days post-infection, tissues, numbers of N'Dama (NDAM) and Boran (BORA) samples, and sources of microarray data used in this study before and after sample filtering.

Days post-infection	Tissue	No. NDAM samples pre-filtering	No. BORA samples pre-filtering	No. NDAM samples post-filtering	No. BORA samples post-filtering	Source*
0	Blood (PBMC)	5	5	5	5	a
0	Liver	20	20	19	18	b
0	Lymph node	5	5	5	4	b
0	Spleen	5	5	5	4	b
12	Liver	5	5	5	5	b
14	Blood (PBMC)	5	5	5	5	a
15	Liver	5	5	5	5	b
18	Liver	5	5	5	5	b
21	Liver	5	5	5	5	b
21	Lymph node	5	5	4	5	b
21	Spleen	5	5	5	5	b
25	Blood (PBMC)	5	5	5	5	a
26	Liver	5	5	3	5	b
29	Liver	5	5	5	5	b
32	Liver	5	5	5	5	b
34	Blood (PBMC)	5	5	5	5	a
35	Liver	5	5	5	5	b
35	Lymph node	5	5	4	5	b
35	Spleen	5	5	5	5	b
Population total		110	110	105	106	
Total		220		211		

*a this study, b [34].

<https://doi.org/10.1371/journal.pntd.0012882.t001>

The intensity of expression for each sample was visualised both with the raw data and after normalisation using affy (v. 1.80.0), Biobase (v. 2.62.0), dplyr (v. 1.1.2) [63], ggh4x (v. 0.2.4) [64], ggplot2 (v. 3.4.2) [65], ggttext (v. 0.1.2) [66], magrittr (v. 2.0.3) [67], readr (v. 2.1.4) [68], reshape2 (v. 1.4.4) [69], and stringr (v. 1.5.0) [70] with R (v. 4.3.2). Colours were generated from khroma (v. 1.10.0) [55] and viridis (v. 0.6.3) [56]. Informative probe sets were identified and extracted using farms (v. 1.25.0) with R (v. 4.3.2).

Principal component analysis

Principal component analysis (PCA) was performed using limma (v. 3.58.1) [71] with R (v. 4.3.2). The results were visualised using dplyr (v. 1.1.2), ggplot2 (v. 3.4.2), patchwork (v. 1.2.0) [72], and stringr (v. 1.5.0), with R (v. 4.3.2). Colours were generated from khroma (v. 1.10.0) and viridis (v. 0.6.3).

Differential expression analysis

Differential expression analysis was performed using limma (v. 3.58.1) [71] with R (v. 4.3.2). The correlation between samples from the same animal was estimated and included in the linear model [71,73]. The contrast matrix contained 64 contrasts across the two populations, four tissues and 12 time points which included direct (DIRE) contrasts to identify changes in expression in the N'Dama samples relative to the Boran samples ($DIRE_i = N_i - B_i$, where N represents the N'Dama population and B represents the Boran population), N'Dama (NDAM) and Boran (BORA) contrasts to identify changes in expression within the populations relative to time 0 ($NDAM_i = N_i - N_0$; $BORA_i = B_i - B_0$) and response (RESP)

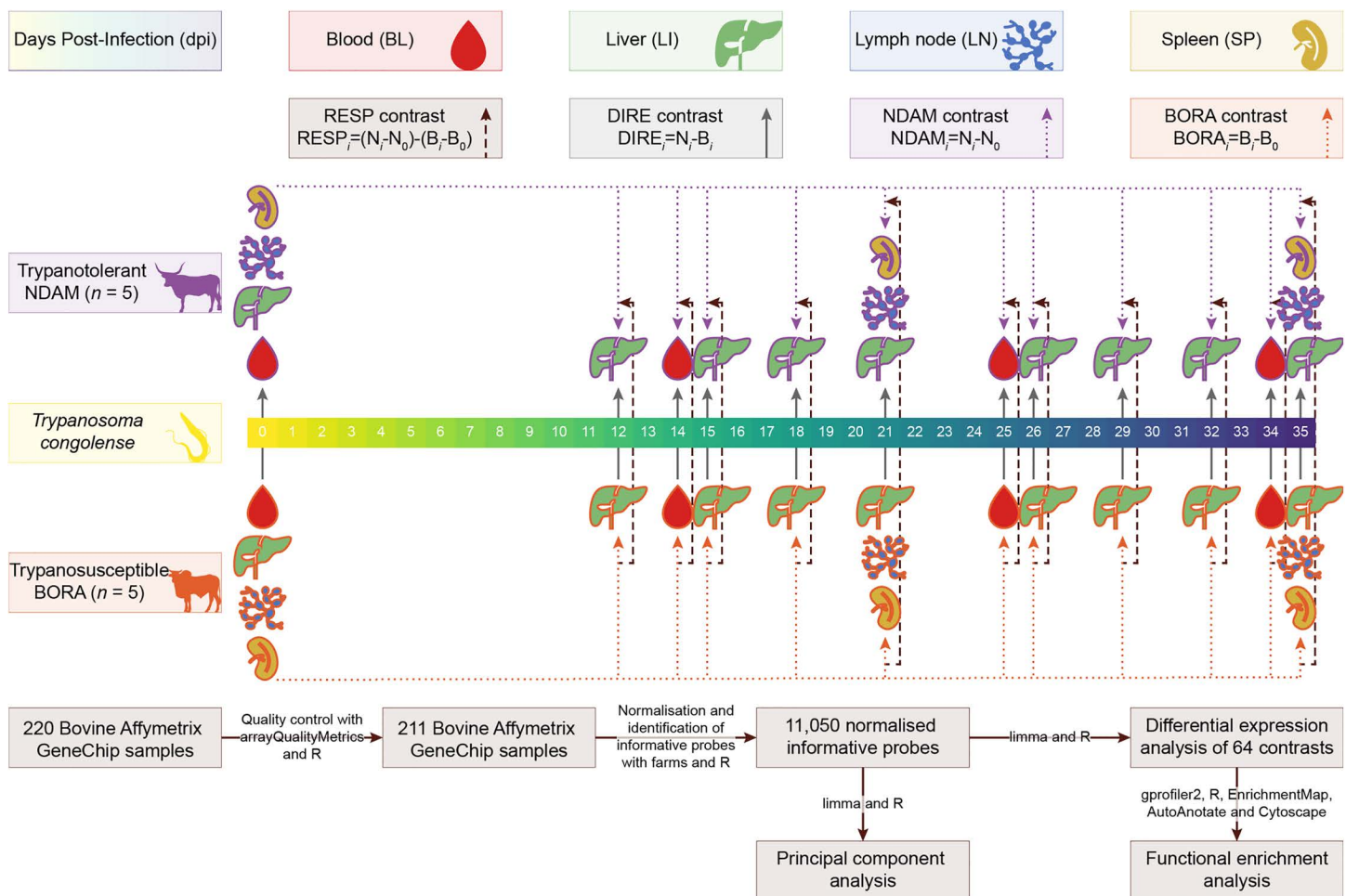


Fig 1. Diagram showing the experimental design and study workflow examining N'Dama (NDAM) and Boran (BORA) cattle. Trypanosome image by Matus Valach and cattle images by Tracy A. Heath and T. Michael Keesey via phylopic.org and tissue images via healthicons.org. Colours were generated from the khroma (v. 1.10.0) [55] and viridis (v. 0.6.3) [56] R packages.

<https://doi.org/10.1371/journal.pntd.0012882.g001>

contrasts to identify changes in expression over time in the N'Dama samples relative to the Boran ($RESP_i = [N_i - N_0] - [B_i - B_0]$) (Fig 1, Table A in S1 Appendix) [34]. The response contrasts represent comparisons between the populations based on the change in expression over time for each population and therefore can detect differences in gene expression between the populations in response to infection rather than baseline differences in expression [34]. Moderated t -statistics, moderated F -statistic, and log-odds of differential expression were calculated for the informative probe sets by empirical Bayes moderation of the standard errors towards a global value [71,74]. Global Benjamini-Hochberg correction for multiple testing was applied across all contrasts [71,75]. Probe sets with an adjusted P -value of ≤ 0.05 (B -H $P_{adj} \leq 0.05$) were determined to be significantly differentially expressed [71]. The microarray probe sets were converted to genes using gprofiler2 (v. 0.2.2) [76] with R (v. 4.3.2).

The results of the differential expression analysis were visualised using ComplexUpset (v. 1.3.3) [77], dplyr (v. 1.1.2), ggh4x (v. 0.2.4), ggplot2 (v. 3.4.2), ggrepel (v. 0.9.3) [78], patchwork (v. 1.2.0), readr (v. 2.1.4), rlang (v. 1.1.1) [79], stringr (v. 1.5.0), and tidyr (v. 1.3.0) [80] with R (v. 4.3.2). Colours were generated from khroma (v. 1.10.0) and viridis (v. 0.6.3).

Functional enrichment analysis

Functional enrichment was performed and visualised using dplyr (v. 1.1.2), ggh4x (v. 0.2.4), ggplot2 (v. 3.4.2), ggrepel (v. 0.9.3), gprofiler2 (v. 0.2.2), magick (v. 2.8.1) [81] with ImageMagick (v. 6.9.12.96) [82], magrittr (v. 2.0.3), purrr (v. 1.0.1) [83], readr (v. 2.1.4), rlang (v. 1.1.1), scales (v. 1.2.1) [84], and stringr (v. 1.5.0) with R (v. 4.3.2). Colours were generated from khroma (v. 1.10.0) and viridis (v. 0.6.3). The background set was the set of informative probe sets with valid Ensembl IDs. The query sets included those that were significantly differentially expression (adjusted P -value ≤ 0.05) for each of the 64 contrasts. The analysis was restricted to Gene Ontology (GO) terms, including GO:Biological Process, GO:Cellular Component, and GO:Molecular Function terms, and driver GO terms were highlighted. Generic Enrichment Map (GEM) files were generated and used as input for EnrichmentMap to combine results for all time points for each contrast type (v. 3.3.6) [85] with Cytoscape (v. 3.8.0) [76,86,87]. AutoAnotate (v. 1.3.5) [88] was used to create clusters of GO terms with genes in common with clusterMaker2 (v. 2.0) [89] and annotate them with appropriate names using WordCloud (v. 3.1.4) [90]. The yFiles Layout Algorithms (v. 1.1.3) method [91] was used to remove overlaps in the networks.

Results

Data remaining after filtering and normalisation

Nine samples were indicated as outliers by two or more of the quality control tests and were therefore removed, leaving 211 samples for analysis (Fig A in [S1 Appendix](#), [Table 1](#)). After normalisation the data were filtered to retain only informative probe sets, which resulted in a data set of 11,050 probe sets or 45.89% of the initial 24,128 probe sets.

Principal component analysis shows the distinction of the liver tissue samples

Based on the top ten principal components (PCs), the first PC explained 82.86% of the total variation in the data for PC1–10 and separated the liver from the blood, lymph node, and spleen samples (Fig 2). The second PC explained a further 9.10% of the total variation for PC1–10 and separated the blood from the lymph node and spleen samples (Fig 2). The third and fourth PCs explained 2.24% and 1.78% of the total variation for PC1–10, respectively, and separated the samples according to days post-infection (dpi) while the fifth PC, which explained 1.32% of the total variation in the data for PC1–10 separated the lymph node and spleen samples (Figs B–D in [S1 Appendix](#)).

Differential expression analysis shows peaks of gene expression differences and overlapping differentially expressed genes

The results of the differential expression analysis are detailed in [S1 Table](#) and the number of significant (B-H $P_{adj.} \leq 0.05$) differentially expressed genes (DEGs) generally increased over time across all contrast types and tissues until 21 dpi when they began to decrease slightly before rising again to their peak at 34 or 35 dpi (Fig 3, Figs E–I in [S1 Appendix](#)). The highest numbers of significant DEGs were found in the N'Dama and Boran contrasts, followed by the direct contrasts (Fig 3, Fig E in [S1 Appendix](#)). Within the response contrasts, which represent comparisons between the populations based on the change in expression over time and therefore detect differences in gene expression between the populations in response to infection [34], the highest number of significant DEGs were found in the lymph node samples at 35 dpi (Fig 3, Fig F in [S1 Appendix](#)) while the blood samples at 34 dpi had the highest number of significant DEGs in the direct contrasts (Fig 3, Fig G in [S1 Appendix](#)). The highest number of significant DEGs in the N'Dama and Boran contrasts were at 35 dpi in the lymph node and liver samples, respectively (Fig 3, Figs H and I in [S1 Appendix](#)). The numbers of significant DEGs were generally higher in the N'Dama contrasts than in the Boran contrasts early in the time course (Fig 3, Fig E in [S1 Appendix](#)).

The N'Dama and Boran contrasts also had a higher number of significant DEGs in common between them when overlaps among all 64 contrasts were examined (Fig J in [S1 Appendix](#)). Within the response and direct contrasts any overlaps

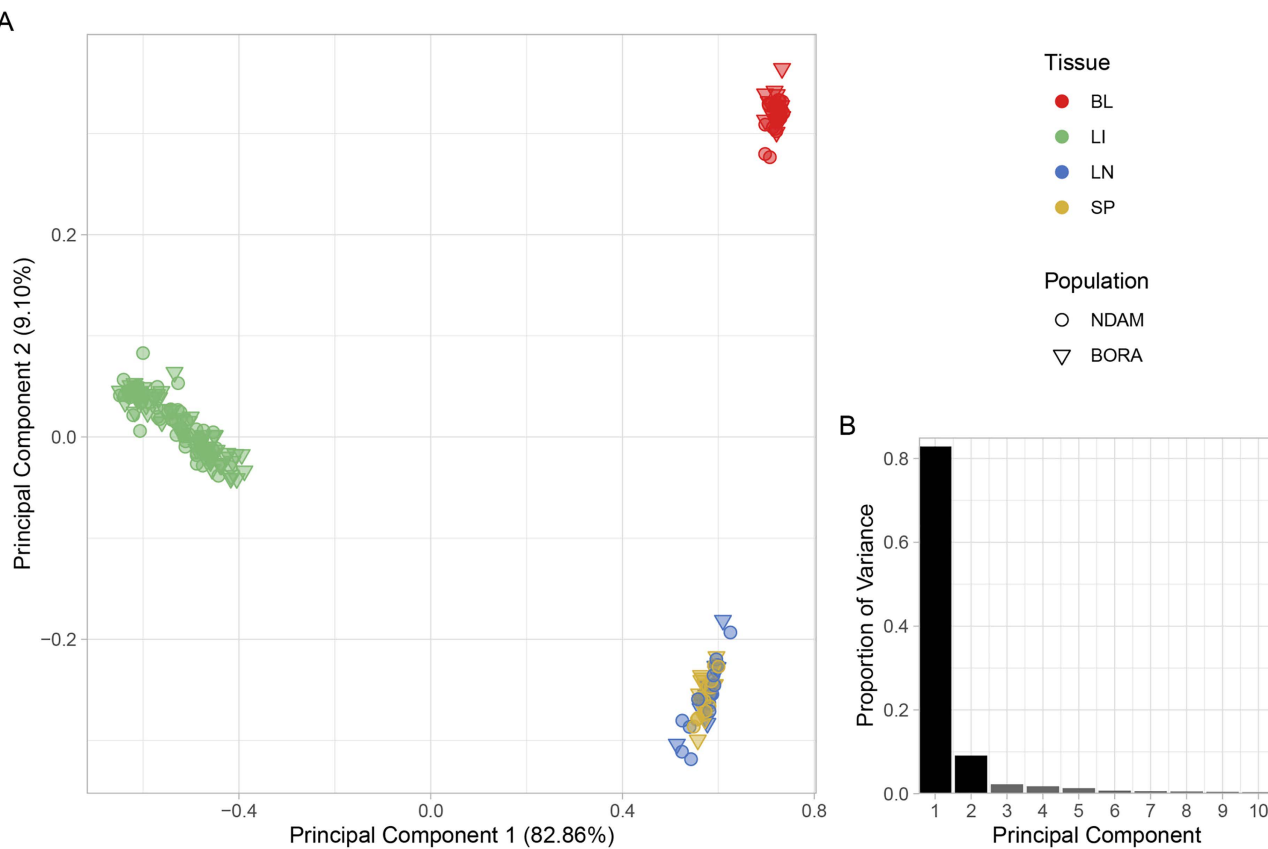


Fig 2. A. Principal component analysis (PCA) of the microarray data set with samples coloured according to tissue, which include blood (BL), liver (LI), lymph node (LN), and spleen (SP) samples, and with the shape indicating the population, which include N'Dama (NDAM) and Boran (BORA) cattle. The first two principal components (PC1 and PC2) are shown, and B. bar chart of proportion of variance of the top ten PCs.

<https://doi.org/10.1371/journal.pntd.0012882.g002>

in significant DEGs were generally confined to those between samples from the same tissue type at different time points (Figs K, L in [S1 Appendix](#)) while the N'Dama and Boran contrasts included more overlaps between tissues and time points (Figs M, N in [S1 Appendix](#)).

There were also many overlaps when the top 10 most significant genes with increased and decreased expression were examined for each of the contrasts ([Table 2](#), Tables B–D in [S1 Appendix](#), [Fig 4](#), Figs O–AB in [S1 Appendix](#)). The set of 1,267 genes identified as being in the top 10 most significant for increased or decreased expression for each of the 64 contrasts contained just 602 unique genes ([Table 2](#), Figs B–D in [S1 Appendix](#)). Of these, 328 were in the top 10 most significant for only one contrast, with the remaining 274 in the top 10 most significant for an average of 3.43 contrasts ([Table 2](#), Tables B–D in [S1 Appendix](#)). The response contrasts had the most unique genes in the top 10 most significant with 129 of the 328 unique top genes, while the direct, N'Dama and Boran contrasts had 75, 58 and 66 unique top genes, respectively ([Table 2](#), Tables B–D in [S1 Appendix](#)). The most common genes in the top 10 most significant differentially expressed for all the contrasts included *TMSB10*, which was in the top 10 most significant genes for 16 of the 64 contrasts, followed by *CYRIB*, *PTPRC*, *SPI1*, and *TTLL1*, which were in the top 10 most significant genes for 14 of the 64 contrasts ([Table 2](#), Tables B–D in [S1 Appendix](#)). The *TMSB10* gene was in the top 10 most significant genes with increased expression for the liver samples at all time points for the N'Dama and Boran contrasts (Tables C, D in [S1 Appendix](#)). The *CYRIB*, *PTPRC*, and *SPI1* genes showed similar patterns with the exclusion of 12 dpi (Tables C, D in [S1 Appendix](#)).

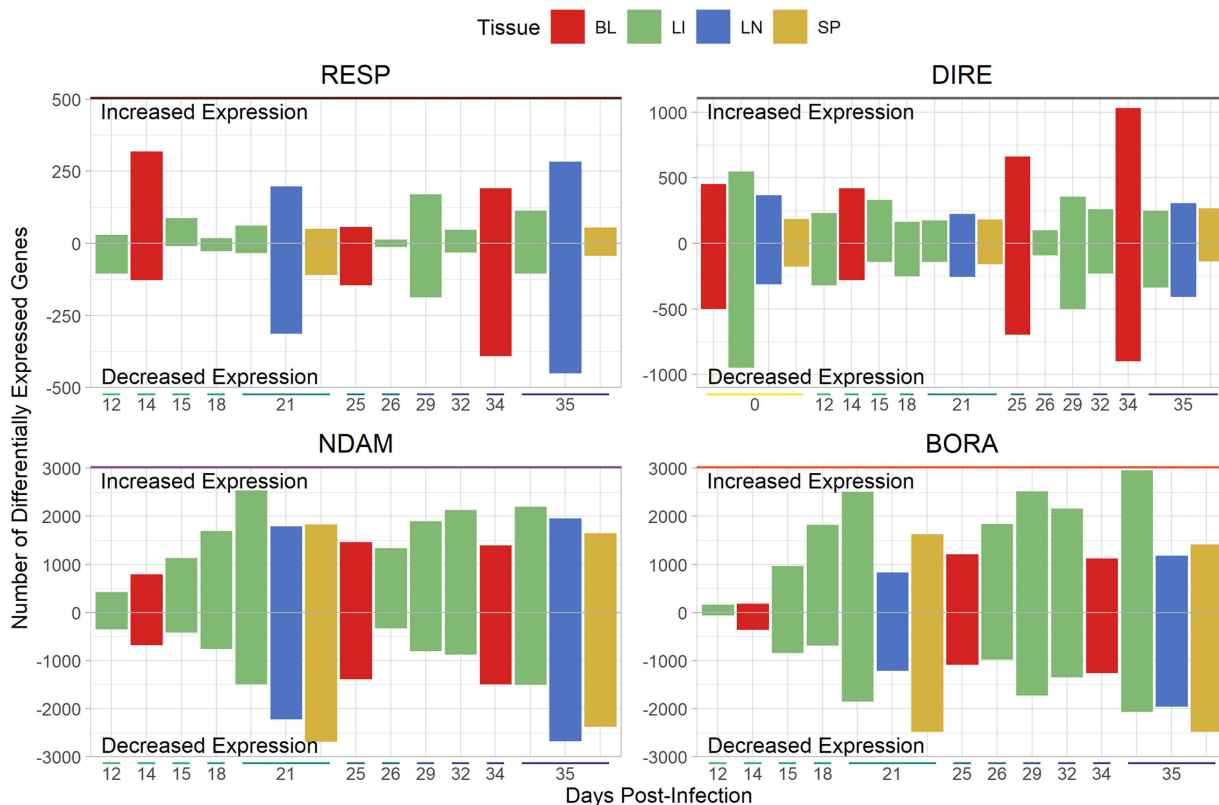


Fig 3. Bar charts showing the numbers of significantly differentially expressed genes for the different contrasts. The extent of the bar above and below 0 on the vertical axis indicates the numbers of significantly differentially expressed genes (DEGs; $B-H P_{adj} \leq 0.05$) with increased and decreased expression, respectively. The position on the horizontal indicates the number of days post-infection (dpi) and the colour of the bars represents the tissue. The direct (DIRE) contrasts identify changes in expression in the N'Dama samples relative to the Boran samples ($DIRE_i = N_i - B_i$, where N represents the N'Dama population and B represents the Boran population), the N'Dama (NDAM) and Boran (BORA) contrasts identify changes in expression within the populations relative to time 0 ($NDAM_i = N_i - N_0$; $BORA_i = B_i - B_0$), and the response (RESP) contrasts identify changes in expression over time in the N'Dama samples relative to the Boran ($RESP_i = [N_i - N_0] - [B_i - B_0]$). The tissues include blood (BL), liver (LI), lymph node (LN), and spleen (SP) samples.

<https://doi.org/10.1371/journal.pntd.0012882.g003>

Appendix). *TTLL1* was in the top 10 most significant genes with increased expression in the blood samples at 25 and 34 dpi and the liver samples at 18 dpi for the response contrasts (Table 2). It was also in the top 10 most significant genes with increased expression for the blood samples at 0, 14, 25, and 34 dpi, the liver samples at 18 dpi, and the lymph node and spleen samples at 0, 21, and 35 dpi for the direct contrasts (Table B in S1 Appendix).

The most common genes in the top 10 most significant differentially expressed for the response contrasts, which represent comparisons between the populations based on the change in expression over time and therefore detect differences in gene expression between the populations in response to infection [34], included *CYP4B1* and *RAB31*, which were in the top 10 most significant genes for four of the 15 response contrasts, followed by *OLFM4*, *TMEM45B*, and *TTLL1*, which were in the top 10 most significant genes for three of the 15 response contrasts (Table 2). For the response contrasts, *CYP4B1* was in the top 10 most significant genes with increased expression for the spleen samples at 21 and 35 dpi and the top 10 most significant genes with decreased expression for the lymph node samples at the same time point contrasts (Table 2). It was also in the top 10 most significant genes with increased expression for the spleen samples at 0 dpi and the top 10 most significant genes with decreased expression for the lymph node samples at the same time point for the direct contrasts (Table B in S1 Appendix). *RAB31* was only in the top 10 most significant genes with decreased expression

Table 2. Tissue, days post-infection (dpi) and the top 10 most significant genes with increased and decreased expression with valid gene symbols for the response contrasts.

Tissue	Days post-infection	Most significant genes with increased expression
BL	14	SRSF11, SNORD50B, CCAR1, RESF1, CLECL1P, KTN1, SENP6, KRR1, CCNL1, TRMT13
BL	25	RESF1, TTLL1, ADAMDEC1, COX6C, KLF5, S100A7, TLR6, CHIC2, ZNF318, RUM1
BL	34	CHIC2, TTLL1, SPDEF, PLAU, CDADC1, SNORD26, SNORD27, MRPL57, POLB, ZC3H12A
LI	12	IL18BP, FOXA3, CXCL11, DVL1, REG3A, CD40, BIRC3, SRGN, MAPK12, WARS1
LI	15	SGCB, RNF39, ITIH2, FBXO34, GNPAT, TCF20, bta-mir-2442, C8H9orf64, SCRNN, STAG2
LI	18	PCF11, TTLL1, PER1, NRG2, CIPC, MKNK2, BAG3, RPL22, ACTR8
LI	21	TMEM45B, RFTN1, UPF2, TCEA3, LTB, CPQ, PLIN5, ABCC5, OSGIN1, SMARCA2
LI	26	TMEM45B, CIDEA, ECT2L, CCDC191, RETSAT, PMVK, CA5A, ANP32A
LI	29	MAGI3, TMEM45B, NGFR, PPP2R5A, CBS, DPYS, MTMR4, UGT2B10, COLEC11, GSTA4
LI	32	SFRP2, APLNR, PLAC8B, CYP3A28, AAMDC, ST7L, MSMO1, SQLE, CES1, TCEA3
LI	35	CES1, RETSAT, CYP3A28, MTMR4, KCNK17, ABHD14B, ACP6, SYBU, ACY1, GCDH
LN	21	ALB, CXCL13, ATP6V0D2, EAF2, SUCLG1, ORC1, SNORA73, ECRG4, SKA2, TNFSF13B
LN	35	CCL20, RGS13, DEFB4A, MYB, ELL3, SNORA73, LNX, PLEKHF2, EED, SPAG5
SP	21	TRMT10B, CYP4B1, NXPH1, KCNA3, MDK, KIRREL2, PTGDS, FAM83D, PRR5L, LTB
SP	35	CYP4B1, MAB21L1, FAM83D, IKZF2, SNCA, PRR5L, RNASE4, RGS13, ZCCHC17, TARP
Tissue	Days post-infection	Most significant genes with decreased expression
BL	14	OLFM4, PGA5, CDC42EP3, ORAI3, KAT7, VAT1L, PMF1, OASL, RAVER1, ICAM3
BL	25	SLC6A4, OLFM4, PGA5, SMOX, PRDM1, SLC9A6, PFKFB4, CCR7, MEIS1, F11R
BL	34	CCR7, ENDOD1, SLC6A4, PIM2, OLFM4, SMOX, TUBB1, ITGA2, DSTN, SLC40A1
LI	12	NUDT12, APOB, PLD1, MYO1B, IQGAP2, CRYZ, EPS8, MASP1, APC, CYP4V2
LI	15	MAPK6, TCIRG1, CXCL17, CUL1, XRN2
LI	18	MEP1B, SLC1A3, TJP2, OLR1, ACTG1, bta-mir-3533, IGFALS, NAE1, IMPA1, SNX6
LI	21	LEAP2, C15H11orf52, SLC25A25, ABHD10, ANGPTL8, LPAR6, KBTBD6, MTRF1, MFSD2A, ISG12(B)
LI	26	PAMR1, RAB31, VLDLR, GPLD1
LI	29	PEG3, RAB31, JCHAIN, WWOX, OTULINL, DNMT1, OLR1, ACTG1, bta-mir-3533, PLTP
LI	32	MEP1B, SLC1A3, JCHAIN, RPSA, SNORA62, XRCC5, RAB31, LDHA, WWOX, CORO1B
LI	35	ANGPTL8, RAB31, LEAP2, ANGPTL4, VLDLR, PLD2, BNIP3, GNL2, MTMR11, S100A8
LN	21	CLDN11, STAB1, CYP4B1, BRB, P2RX4, PROS1, KANK3, HYAL2, ELOVL7, COLEC12
LN	35	BRB, CYP4B1, STAB1, CLDN11, PROS1, HEPH, P2RX4, MAN1C1, C1QTNF5, SCARA5
SP	21	BMP2, FABP3, GRO1, THBS1, BCL10, F2RL2, CLDN1, SAMS1, TLR4, ARL14EP
SP	35	NELL2, CD14, ITGA8, MUSTN1, RBP1, F2RL2, CXCL16, IL33, CATHL3, BMP2

<https://doi.org/10.1371/journal.pntd.0012882.t002>

for the liver samples at 26, 29, 32, and 35 dpi for the response contrasts (Table 2). For the response contrasts, *OLFM4* was in the top 10 most significant genes with decreased expression for the blood samples at 14, 25, and 34 dpi (Fig 4, Table 2). It was also in the top 10 most significant genes with decreased expression for the blood samples at 0 dpi for the direct contrasts, and at 14, 25, and 34 dpi for the N'Dama contrasts (Tables B and C in S1 Appendix). For the response contrasts, *TMEM45B* was in the top 10 most significant genes with increased expression for the liver samples at 21, 26, and 29 dpi (Table 2). It was also in the top 10 most significant genes with decreased expression for the liver samples at 0, 12, and 15 dpi for the direct contrasts (Table B in S1 Appendix).

Functional enrichment analysis shows enriched networks of related GO terms

GO terms related to regulation of the mitotic cell cycle were significantly enriched for the genes with significantly increased expression in the blood and lymph node samples for the response contrasts (Fig 5). The top driver GO terms for the

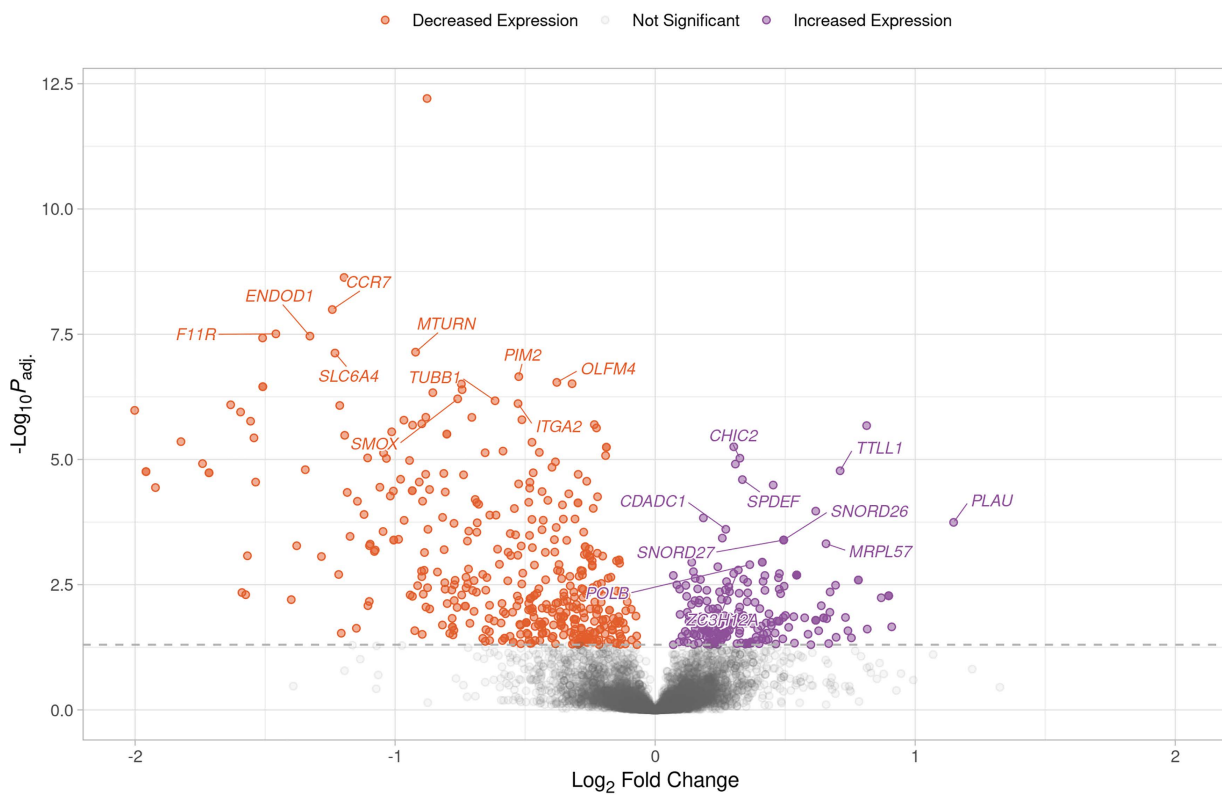


Fig 4. Volcano plot showing the results of the RESP contrast for the peripheral blood mononuclear cell (PBMC) samples at 34 days post-infection (dpi). Each data point represents a gene with the position on the x- and y-axes indicating the \log_2 fold change and $-\log_{10} P_{\text{adj}}$, respectively. Genes above the horizontal dashed line are significantly differentially expressed with the colours representing the change in expression. The top 10 most significant genes for increased and decreased expression with gene symbols are labelled.

<https://doi.org/10.1371/journal.pntd.0012882.g004>

blood samples included GO:0006396 RNA processing and GO:0005730 nucleolus (Fig AC in [S1 Appendix](#)) while the top driver GO terms for the lymph node samples included GO:0007059 chromosome segregation, GO:0005694 chromosome, GO:0006259 DNA metabolic process, GO:0006260 DNA replication, GO:0051301 cell division, GO:0003677 DNA binding, and GO:0008017 microtubule binding (Fig AD in [S1 Appendix](#)). GO terms related to steroid metabolic processes (GO:0008202 steroid metabolic process) and oxidoreductase activity (GO:0016705 oxidoreductase activity, acting on paired donors, with incorporation or reduction of molecular oxygen, GO:0016712 oxidoreductase activity, acting on paired donors, with incorporation or reduction of molecular oxygen, reduced flavin or flavoprotein as one donor, and incorporation of one atom of oxygen) were significantly enriched for the genes with significantly increased expression in the liver samples for the response contrasts (Fig 5, Fig AE in [S1 Appendix](#)). No GO terms were significantly enriched for genes with significantly increased expression in the spleen samples for the response contrasts (Fig 5).

When all time points were combined, GO terms related to blood coagulation (GO:0007596 blood coagulation) and the cell-substrate junction (GO:0030055 cell-substrate junction) were significantly enriched for the genes with significantly decreased expression in the blood samples for the response contrasts, which represent comparisons between the populations based on the change in expression over time and therefore detect differences in gene expression between the populations in response to infection [34] (Fig 5, Fig AC in [S1 Appendix](#)). GO terms related to receptor-mediated endocytosis were significantly enriched for the genes with significantly decreased expression in the liver and lymph node samples for the response contrasts (Fig 5). The top driver GO terms included GO:0003823 antigen binding for the liver samples

(Fig AE in [S1 Appendix](#)), and GO:0071944 *cell periphery*, GO:0009986 *cell surface*, GO:0007155 *cell adhesion*, and GO:0006897 *endocytosis* for the lymph node samples (Fig AD in [S1 Appendix](#)). GO terms related to multicellular development and morphogenesis including the driver GO terms GO:0007167 *enzyme-linked receptor protein signalling pathway*, GO:0032501 *multicellular organismal process*, and GO:0071495 *cellular response to endogenous stimulus* were also significantly enriched for the genes with significantly decreased expression in the lymph node samples for the response contrasts (Fig 5, Fig AD in [S1 Appendix](#)). GO terms related to cell migration and motility (GO:0016477 *cell migration*, GO:0048870 *cell motility*) and cargo receptor activity (GO:0038024 *cargo receptor activity*) were also enriched for these genes (Fig 5, Fig AD in [S1 Appendix](#)). GO terms related to the extracellular region (GO:0005576 *extracellular region*) were significantly enriched for the genes with significantly decreased expression in both the lymph node and spleen samples for the response contrasts (Fig 5, Fig AD, AF in [S1 Appendix](#)), while GO terms related to lipopolysaccharide binding (GO:0001530 *lipopolysaccharide binding*) were also significantly enriched for the genes with significantly decreased expression in the spleen samples for the response contrasts (Fig 5, Fig AF in [S1 Appendix](#)).

When all time points were combined for the direct contrasts, GO terms related to organelle metabolic processes were significantly enriched for the genes with significantly increased expression in the blood, liver, and lymph node samples (Fig AG in [S1 Appendix](#)). The GO term for leukocyte proliferation was significantly enriched for genes with significantly increased expression in the blood samples, while GO terms related to scavenger receptor activity and cell periphery were also significantly enriched for genes with significantly increased expression in the lymph node samples (Fig AG in [S1 Appendix](#)). GO terms related to receptor signalling pathways were significantly enriched for genes with significantly decreased expression in the liver and lymph node samples, while GO terms related to coagulation were significantly enriched for genes with significantly decreased expression in the blood samples (Fig AG in [S1 Appendix](#)). GO terms related to actin binding and cytoskeleton, immune response and antigen binding, small molecule and pyruvate metabolic processes, and the cytosolic ribosome were also significantly enriched for genes with significantly decreased expression in the liver samples (Fig AG in [S1 Appendix](#)). GO terms related to tube development, cell migration, extracellular region, cell adhesion, and calcium ion binding were significantly enriched for genes with significantly decreased expression in the lymph node samples (Fig AG in [S1 Appendix](#)). GO terms related to metaphase chromosome alignment, the chromosome centromeric region, and the microtubule cytoskeleton were significantly enriched for genes with significantly decreased expression in the spleen samples (Fig AG in [S1 Appendix](#)).

When all time points were combined for the N'Dama contrasts, GO terms related to cell process regulation were significantly enriched for genes with significantly increased expression in all tissues (Fig AH in [S1 Appendix](#)). GO terms related to GTPase activator activity, phagocytosis, and protein kinase binding were also significantly enriched for genes with significantly increased expression in the liver samples (Fig AH in [S1 Appendix](#)). GO terms related to cell development and regulation were significantly enriched for genes with significantly decreased expression in all tissues (Fig AH in [S1 Appendix](#)). GO terms related to metabolic processes, peroxisome organization, electron transfer activity, oxidoreductase activity, and the endoplasmic reticulum membrane were enriched for genes with significantly decreased expression in the liver samples (Fig AH in [S1 Appendix](#)). GO terms related to actin cytoskeleton organization, extracellular matrix, cell projection, and vesicle-mediated transport were significantly enriched for genes with significantly decreased expression in the lymph node and spleen samples (Fig AH in [S1 Appendix](#)). GO terms related to the extracellular region were also significantly enriched for genes with significantly decreased expression in the lymph node samples, while GO terms related to extracellular matrix organization were significantly enriched for genes with significantly decreased expression in the spleen samples (Fig AH in [S1 Appendix](#)). When all time points were combined for the Boran contrasts, GO terms related to cell process regulation were significantly enriched for genes with significantly increased expression in all tissues and GO terms related to cell response regulation were significantly enriched for genes with significantly decreased expression in all tissues, while GO terms related to metabolic processes were also significantly enriched for genes with significantly decreased expression in the liver and spleen samples (Fig AI in [S1 Appendix](#)).

Expression  Increased  Decreased Tissue  BL  LI  LN  SP

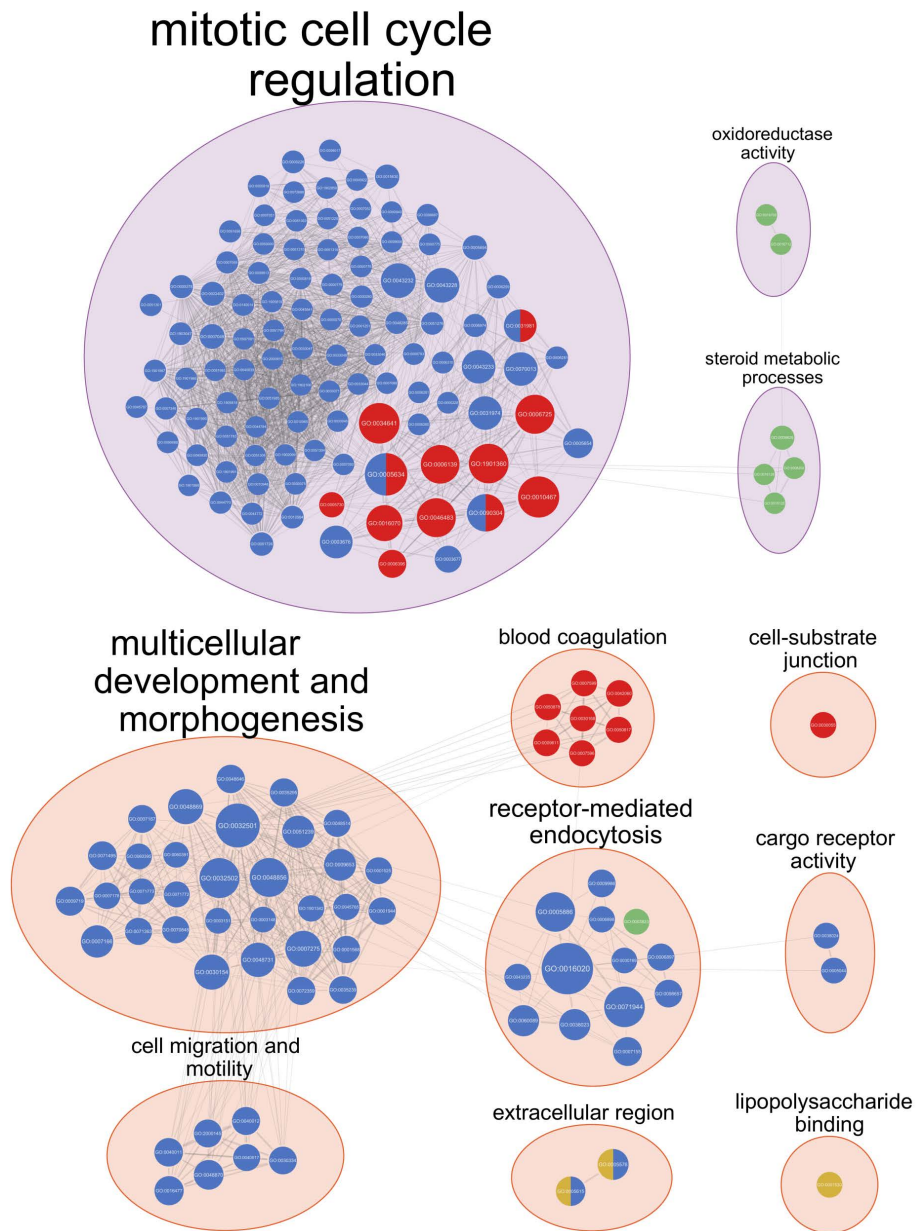


Fig 5. EnrichmentMap network of significantly enriched gene ontology (GO) terms identified from g:Profiler functional enrichment of significantly differentially expressed genes (DEGs) for the response contrasts at all time points. Each node represents a GO term with the colour of the node representing the tissue and the size representing the number of genes in the GO term. The edges indicate overlap between the GO terms with the width of the edges representing the similarity coefficient for the connected GO terms. The GO terms are clustered by AutoAnnotate with the background colour of the clusters representing the direction of expression. The clusters are labelled with the size of the label scaling with the number of GO terms in the cluster.

<https://doi.org/10.1371/journal.pntd.0012882.g005>

Discussion

The data filtering and normalisation steps resulted in a similar number of samples and probe sets for analysis as previous studies that used Affymetrix Bovine Genome Array data sets to examine host responses to trypanosomiasis and other infectious diseases of cattle, including the previous analysis of the liver, lymph node, and spleen samples [34,92–94]. The clear separation of the liver samples from the other tissues that is evident for PC1, which also explained the majority of the total variation in the data set for PC1–10, may be due to several factors (Fig 2). The first is biological differentiation between the liver samples and those of the other tissues. This is supported by a previous gene expression microarray study using rat (*Rattus norvegicus*) tissues, which also observed that PC1 in a PCA separated liver samples from those taken from blood, lymph node, spleen, and other tissues [95]. This biological difference may have been compounded by the higher number of liver samples in the data set from Noyes and colleagues [34] due to the experimental design, which encompassed a larger number of time points for the liver samples as well as a greater number of animals from which the liver samples were taken to prevent the collection of multiple liver biopsies from the same animal at consecutive time points [34]. This experimental design consideration also resulted in more control liver samples for the pre-infection time point [34]. In total, 115 of the 211 samples that passed the quality control filters or 54.50% of the filtered data set were liver samples (Table 1). Because an unequal number of samples is known to increase the distance between groups with larger sample sizes in a PCA, it is possible that the disproportionately large number of liver samples in the present study has given rise to the effect seen in PC1 [96–98]. It is therefore unsurprising that PC2, which explained a further 9.10% of the total variation in the data set for PC1–10, separated the blood samples from the lymph node and spleen samples (Fig 2) as the blood samples were the second most numerous in the data set with 40 samples or 18.96% of the filtered data set (Table 1). It is not until PC5, which explained 1.32% of the total variation in the data set for PC1–10, that the lymph node and spleen samples are separated (Fig D in S1 Appendix). The samples from these tissues are the least numerous in the data set with 29 spleen and 27 lymph node samples, making up 13.74% and 12.80% of the filtered data set, respectively (Table 1). The spleen and lymph nodes are also both key components of the lymphatic and immune systems and their functional and morphological similarities as hemopoietic organs that filter bodily fluids have been long established [99–101]. It is logical, therefore, that these tissues would show similar patterns of gene expression both before and after infection. The third and fourth PCs (PC3 and PC4), which explained 2.24% and 1.78% of the total variation for PC1–10, respectively, separated the samples temporally in order of dpi (Figs B, C in S1 Appendix). This illustrates the overall similarity in response to infection across the populations and is in agreement with RNA-seq data from whole blood samples taken during a similar trypanosome infection time course experiment [43]. It also shows that the systemic response to trypanosome infection in peripheral blood is distinct from that in the liver and other tissues and that blood sampling alone may not be sufficient to capture all the tissue specific responses to infection.

Gene expression in bovine tissues can be measured using a variety of methods, one of which is the Affymetrix Bovine Genome Array based on GeneChip technology [102] and which contains more than 24,000 probe sets representing over 23,000 gene transcripts. The Affymetrix Bovine Genome Array platform has been previously used to study infectious disease in cattle, including trypanosomiasis [34], and for mycobacterial infections that cause tuberculosis and paratuberculosis [92–94]. Importantly, although expression microarrays have been largely supplanted by RNA sequencing (RNA-seq), when the same biological samples were analysed using both the Bovine Genome Array and RNA-seq, gene expression data obtained using the two platforms were extremely well correlated in peripheral blood and alveolar macrophages [103–105]. In addition, it has recently been shown that peripheral blood gene expression data generated using RNA-seq, a different microarray technology (long oligonucleotide microarrays), and reverse transcription quantitative real-time PCR (RT-qPCR) were well correlated in independent studies of trypanosome infection in cattle [43].

The pattern of an increase in the numbers of significant DEGs until 21 dpi followed by a decrease before rising to a final peak at 35 dpi across contrast types and tissues (Fig 3, Figs E–I in S1 Appendix) is consistent with known information about the cyclic nature of parasitaemia during trypanosome infection, which has been shown to have an initial peak

at 20 dpi [39]. It is also in agreement with the measures of parasitaemia in the blood samples during this infection time course experiment, which showed peaks of parasitaemia from 15 to 22 dpi [42]. The final peak of significant DEGs at the end of the infection time course is consistent with analysis of the same blood samples using a gene expression platform with less gene content—a bovine long oligonucleotide (BLO) array—which detected the highest number of significant DEGs between the two populations at 34 dpi [41]. It is also in agreement with a study using RNA-seq data from whole blood samples that found the highest number of DEGs in N'Dama samples at the end of a similar trypanosome infection time course experiment [43]. The higher numbers of significant DEGs in the N'Dama contrasts when compared to the Boran contrasts is in agreement with previous results and supports the hypothesis that, compared to trypanosusceptible Boran, trypanotolerant N'Dama cattle exhibit an earlier proinflammatory response, which is evident in both PBMC and whole peripheral blood [41–43]. That the response contrasts had the lowest number of significant DEGs is to be expected given that these contrasts are examining the data set for differences in the rate of change of gene expression between the populations [34]. In addition, the numbers of significant DEGs for the response contrasts were similar to those found in the original analysis by Noyes and colleagues [34], which employed a similar approach. The numbers of genes in common between the contrasts is to be expected due to the shared underlying data set while the numbers of genes in common within the contrasts is likely due to similar patterns of gene expression found across the populations, tissues, and time points during the infection (Figs J–N in [S1 Appendix](#)). This is in agreement with RNA-seq data that showed large overlaps in DEGs in response to trypanosome infection between five different cattle populations with varying levels of trypanotolerance [43].

The similarities in gene expression are also illustrated by the high level of overlap in the top 10 most significant DEGs with increased and decreased expression between the contrasts ([Table 2](#), Tables B–D in [S1 Appendix](#)). The most common genes in the top 10 most significant DEGs for all the contrasts included those related to the immune system, such as the most common significant DEG—the thymosin beta 10 gene (*TMSB10*), which has been identified as a hub gene in the response to Rift Valley fever (RVF), an important viral disease in African cattle [106]. Other immune-related genes in the set of the most common genes in the top 10 most significant DEGs for all the contrasts included the CYFIP related Rac1 interactor B gene (*CYR1B*), which encodes a regulator of phagocytosis [107], and the protein tyrosine phosphatase receptor type C gene (*PTPRC*), which is an essential regulator of T and B cell antigen receptor-mediated activation and has been highlighted by multiple studies of trypanosome infection in mice [108–113]. Similarly, the Spi-1 proto-oncogene gene (*SPI1*), which encodes a transcription factor that activates gene expression during myeloid and B-lymphoid cell development, has also been implicated as an important host gene in trypanosome infection in the mouse [112,114]. The presence of immune genes in the top 10 most significant DEGs is to be expected given the nature of the infection time course experiment and is in agreement with previous results from this and other infection experiments, illustrating the similarity in immune responses between the N'Dama and Boran cattle during trypanosome infection [34,41,43].

The most common genes in the top 10 most significant DEGs for the response contrasts, which represent comparisons between the populations based on the change in expression over time and therefore detect differences in gene expression between the populations in response to infection [34], included genes which are involved in inflammation and immunity such as the olfactomedin 4 gene (*OLFM4*) and the transmembrane protein 45B gene (*TMEM45B*) [115,116]. Other common genes in the top 10 most significant DEGs for the response contrasts are more varied in function and included the cytochrome P450 family 4 subfamily B member 1 gene (*CYP4B1*), which is involved in drug metabolism [117]; the RAB31, member RAS oncogene family gene (*RAB31*), which is a small GTPase [118]; and the TTL family tubulin polyglutamylase complex subunit L1 gene (*TTLL1*), which is involved in microtubule cytoskeleton organisation [119].

The top 10 most significant DEGs for the response contrasts also included genes encoding antimicrobial peptides (AMPs), which are key components of the innate immune system that have huge therapeutic potential and are important for the healthy function of a variety of bovine tissues [120–123]. This is in agreement with previous RT-qPCR results using blood samples from the same time course infection experiment; in this regard, it has previously been hypothesised that

trypanotolerance may be partly due to inherited regulatory sequence variation in genes encoding antimicrobial peptides [40]. For example, the liver enriched antimicrobial peptide 2 gene (*LEAP2*) [124], which was in the top 10 most significant DEGs with decreased expression for the liver samples at 21 and 35 dpi for the response contrasts (Table 2). The previous RT-qPCR results showed that *LEAP2* exhibited significantly decreased expression in N'Dama samples at 34 dpi relative to day 0 while the Boran animals showed no such change [40]. Other AMP genes in the top 10 most significant DEGs for the response contrasts which examine the N'Dama samples relative to the Boran samples included the cathelicidin antimicrobial peptide gene (*CATHL3*) [125] with decreased expression in the spleen samples at 35 dpi, which is notable since cathelicidins were found to be the most effective of the three classes of AMP at killing both insect and bloodstream forms of *T. brucei* in mice [126]; the defensin beta 4A gene (*DEFB4A*) [127] with increased expression in the lymph node samples at 35 dpi; and S100 calcium binding protein A7 gene (*S100A7*) [128] with increased expression in peripheral blood at 25 dpi (Table 2) [40,125,127,128].

Another group of genes represented in the top 10 most significant DEGs for the response contrasts were cytokine genes (Table 2). This is consistent with both RT-qPCR and BLO microarray results from the same infection time course experiment and previous studies using the same animals [34,41,42]. This observation agrees with more recent transcriptomics studies from trypanotolerant and trypanosusceptible cattle and studies of trypanosome infection in the mouse [43,129]. These genes included the C-C motif chemokine ligand 20 gene (*CCL20*) with increased expression in the lymph node samples at 35 dpi; the C-X-C motif chemokine ligand 11 (*CXCL11*) with increased expression in the liver samples at 12 dpi; the C-X-C motif chemokine ligand 13 gene (*CXCL13*) with increased expression in the lymph node samples at 21 dpi; the C-X-C motif chemokine ligand 16 gene (*CXCL16*) with decreased expression in the spleen samples 35 dpi; the C-X-C motif chemokine ligand 17 gene (*CXCL17*) with decreased expression in the liver samples at 15 dpi; the interleukin 33 gene (*IL33*) with decreased expression in the lymph node samples at 35 dpi; and the TNF superfamily member 13b gene (*TNFSF13B*) with increased expression in the lymph node samples at 21 dpi (Table 2). This is particularly notable in terms of B cell response since genes such as the *CXCL13* gene and the *TNFSF13B* gene are known to act as a B cell chemoattractant and activator, respectively, and both of these genes have been found to be involved in the response to trypanosome infection in mice [130]. B cells play a key role in the humoral response of the host to trypanosome infection [131]. In addition, it is thought that autoimmunity, particularly autoantibodies secreted by atypical B cells that have been found to correlate with anaemia during trypanosome infection, may contribute to anaemia in response to trypanosome infection [132].

Related genes such as cytokine receptors and inhibitors were also in the top 10 most significant DEGs for the response contrasts (Table 2). These included the C-C motif chemokine receptor 7 gene (*CCR7*) with decreased expression in the blood samples at 25 and 34 dpi; the C1q and TNF related 5 gene (*C1QTNF5*) with decreased expression in lymph node samples at 35 dpi; and the interleukin 18 binding protein gene (*IL18BP*) with increased expression in the liver samples at 12 dpi (Table 2). Additionally, mitogen-activated protein kinase (MAPK) genes were present in the top 10 most significant DEGs, which is in agreement with previous work using the same animals and also a more recent study of trypanosome infection in cattle [34,41,43]. In this regard, it is notable that MAPK signalling pathways are involved in the response to proinflammatory cytokines and are known to be subverted by *T. cruzi* and other trypanosomatid parasites to evade the host immune response [133–135].

A final notable group of genes present in the top 10 most significant DEGs were those encoding apolipoproteins, including apolipoprotein B (*APOB*) with decreased expression for the response contrast in the liver samples at 12 dpi (Table 2); apolipoprotein L3 (*APOL3*) with increased expression for the direct contrast in the blood samples at 25 dpi (Table B in S1 Appendix); and apolipoprotein M (*APOM*) with decreased expression for the Boran contrast in the liver samples at 15 dpi (Table D in S1 Appendix). These genes are related to apolipoprotein 1 (*APOL1*) which encodes the protein that makes up the trypanosome lytic factor (TLF) that is present in human and western lowland gorilla (*Gorilla gorilla gorilla*) serum [136]. TLF is taken up by susceptible trypanosomes where it interferes with their lysosomes and mitochondria, thereby

conferring host resistance to most trypanosome species [136]. It is therefore interesting that related genes are among the top 10 most differentially expressed in this study.

Gene ontology terms related to regulation of the mitotic cell cycle, steroid metabolic processes and oxidoreductase activity (Fig 5) were significantly enriched for the genes with significantly increased expression for the response contrasts when all time points were combined, which is in agreement with results from a previous study using the same animals [34]. The overlap and grouping of the GO terms between the blood and lymph node samples illustrates the similarity of responses to infection for these tissues. The lack of GO terms significantly enriched for genes with significantly increased expression for the response contrasts in the spleen samples (Fig 5) can be explained by the lower numbers of significant DEGs with increased expression for these samples (Fig 3, Fig F in S1 Appendix). A larger range of GO terms were significantly enriched for the genes with significantly decreased expression for the response contrasts (Fig 5). This is likely due to the higher number of significant DEGs with decreased expression, which would allow more GO terms to be significantly enriched for these genes (Fig 3). The GO terms significantly enriched for the genes with significantly decreased expression for the response contrasts included those related to multicellular development and morphogenesis, receptor-mediated endocytosis, cell migration and motility, cargo receptor activity, extracellular region, and lipopolysaccharide binding (Fig 5). These observations are also in agreement with results of the previous analysis using the same animals [34].

It is logical that the GO terms that are significantly enriched for genes with significantly decreased expression for the response contrasts are related to blood coagulation in the PBMC samples (Fig 5, Fig AC in S1 Appendix). The effects of blood-borne trypanosome parasites on the blood of the host have been long studied in both cattle and humans [137–139]. Notably, anaemia is the main cause of death due trypanosomiasis and the ability to control this anaemia is considered critical to trypanotolerance in cattle [140,141]. While trypanosomes do obtain iron from their environment in the blood of the host and that iron homeostasis and metabolism in the trypanosome parasite are known to be essential for infection, it has been observed that anaemia does not correlate with parasitaemia [142–145]. Additionally, trypanosomes require much less iron than a mammalian cell [146,147]. The anaemia caused by trypanosome infection is therefore considered to be an immune response, which may be driven by cytokines [141,148,149].

During trypanosome infection in cattle, control of anaemia and parasitaemia are key components of trypanotolerance but are considered to represent separate genetically determined traits [150]. This is exemplified by genes related to iron ion homeostasis such as the solute carrier family 40 member 1 gene (*SLC40A1*) [151], which was noted to be among the most divergent between trypanotolerant N'Dama and trypanosusceptible Boran as a result of a marked reduction in expression in the N'Dama population over the course of the infection experiment relative to the pre-infection level in PBMC [41]. *SLC40A1* was also in the top 10 most significant DEGs with decreased expression in the blood samples at 34 dpi for the response contrast in this study, highlighting the divergent nature of the expression of this gene between the N'Dama and Boran populations during trypanosome infection (Table 2). The reduction of cellular iron export by the *SLC40A1* protein is thought to be a component of an innate immune-driven strategy to prevent bloodstream pathogens from accessing iron, with anaemia as a side effect for the host [141,144,148]. A related gene, the solute carrier family 11 member 1 gene (*SLC11A1*), which regulates iron homeostasis in macrophages was found to be differentially expressed between N'Dama and African indicine cattle during trypanosome infection using RNA-seq data [43] and variants of this gene are associated with susceptibility to several infectious diseases, including tuberculosis in cattle [152,153]. Finally, it is noteworthy that the previous work by Noyes and colleagues [34], which used a different functional enrichment approach also highlighted biological pathways related to iron ion homeostasis.

The significantly enriched GO terms showed similar patterns for the direct contrasts with those enriched for the genes with significantly increased expression related to organelle metabolic processes for multiple tissues, while those enriched for the genes with significantly decreased expression showed a greater range of processes (Fig AG in S1 Appendix). Gene ontology terms related to coagulation were also significantly enriched for genes with significantly decreased expression in the PBMC samples (Fig AG in S1 Appendix). For the N'Dama and Boran contrasts, the significantly enriched GO

terms were related to cell regulation across all tissues, time points, and direction of expression (Figs AH, AI in [S1 Appendix](#)). This is likely a result of the higher numbers of significant DEGs for these contrasts, which led to higher numbers of significantly enriched GO terms that were too varied for the EnrichmentMap method to summarise effectively ([Fig 3](#)) [85].

In conclusion, trypanotolerant N'Dama and trypanosusceptible Boran cattle responded in largely similar ways during trypanosome infection when gene expression was examined using PBMC, liver, lymph node, and spleen samples with peaks and troughs of gene expression following the cyclic pattern of parasitaemia exhibited during trypanosome infection. Differences in response to infection between the two populations include genes related to the immune system such as those encoding antimicrobial peptides and cytokines. Within the PBMC samples, differences in genes relating to coagulation and iron homeostasis support the hypothesis that the dual abilities to control both parasitaemia and the anaemia resulting from the innate immune response to trypanosome parasites are key to trypanotolerance. This work adds to our understanding of host-trypanosome interactions across multiple tissues and time points as well as to our knowledge of how genetic variation underlying the host response can lead to differential host tolerance of, or susceptibility to, trypanosome infection. This improves our general understanding of mammalian trypanosome infection which may also be applicable to human African trypanosomiasis.

Supporting information

S1 Appendix. Supporting information for Functional genomics of trypanotolerant and trypanosusceptible cattle infected with *Trypanosoma congolense* across multiple time points and tissues.
(DOCX)

S1 Table. Differential expression analysis results including the probe ID, gene ID, log₂ fold change, and *P*_{adj.} for each of the 64 contrasts.
(XLSX)

Acknowledgments

We thank Morris Agaba, Olivier Hanotte, Stephen J. Kemp, and Stephen V. Gordon for assistance with sample resources and for useful scientific discussion.

Author contributions

Conceptualization: Gillian P. McHugo, Grace M. O'Gorman, Kieran G. Meade, Emmeline W. Hill, David E. MacHugh.

Data curation: Gillian P. McHugo, John A. Browne, Grace M. O'Gorman, Thomas J. Hall.

Formal analysis: Gillian P. McHugo, James A. Ward, Grace M. O'Gorman, Emmeline W. Hill, David E. MacHugh.

Funding acquisition: David E. MacHugh.

Investigation: Gillian P. McHugo, James A. Ward, John A. Browne, Grace M. O'Gorman, Kieran G. Meade, Emmeline W. Hill, Thomas J. Hall, David E. MacHugh.

Methodology: Gillian P. McHugo, James A. Ward, John A. Browne, Grace M. O'Gorman, Kieran G. Meade, Emmeline W. Hill, Thomas J. Hall, David E. MacHugh.

Project administration: Emmeline W. Hill, David E. MacHugh.

Resources: John A. Browne, Grace M. O'Gorman, Kieran G. Meade, Emmeline W. Hill, Thomas J. Hall, David E. MacHugh.

Software: Gillian P. McHugo, James A. Ward, Thomas J. Hall.

Supervision: John A. Browne, Emmeline W. Hill, Thomas J. Hall, David E. MacHugh.

Visualization: Gillian P. McHugo, James A. Ward.

Writing – original draft: Gillian P. McHugo, James A. Ward, John A. Browne, Emmeline W. Hill, Thomas J. Hall, David E. MacHugh.

Writing – review & editing: Gillian P. McHugo, Grace M. O’Gorman, Kieran G. Meade, David E. MacHugh.

References

1. Steverding D. The history of African trypanosomiasis. *Parasit Vectors*. 2008;1(1):3. <https://doi.org/10.1186/1756-3305-1-3> PMID: 18275594
2. Brun R, Blum J, Chappuis F, Burri C. Human African trypanosomiasis. *Lancet*. 2010;375(9709):148–59. [https://doi.org/10.1016/S0140-6736\(09\)60829-1](https://doi.org/10.1016/S0140-6736(09)60829-1) PMID: 19833383
3. Taylor KA. Immune responses of cattle to African trypanosomes: protective or pathogenic?. *Int J Parasitol*. 1998;28(2):219–40. [https://doi.org/10.1016/s0020-7519\(97\)00154-9](https://doi.org/10.1016/s0020-7519(97)00154-9) PMID: 9512986
4. Taylor KA, Mertens B. Immune response of cattle infected with African trypanosomes. *Mem Inst Oswaldo Cruz*. 1999;94(2):239–44. <https://doi.org/10.1590/s0074-02761999000200022> PMID: 10224536
5. Ibrahim MAM, Weber JS, Ngomtcho SCH, Signaboubo D, Berger P, Hassane HM, et al. Diversity of trypanosomes in humans and cattle in the HAT foci Mandoul and Maro, Southern Chad—A matter of concern for zoonotic potential?. *PLoS Negl Trop Dis*. 2021;15(6):e0009323. <https://doi.org/10.1371/journal.pntd.0009323> PMID: 34106914
6. Houyèmè RE, Kaboré J, Gimonneau G, Somda MB, Salou E, Missihoun AA, et al. Molecular epidemiology of Animal African Trypanosomosis in southwest Burkina Faso. *PLoS Negl Trop Dis*. 2022;16(8):e0010106. <https://doi.org/10.1371/journal.pntd.0010106> PMID: 35994491
7. N'Djetchi MK, Ilboudo H, Koffi M, Kaboré J, Kaboré JW, Kaba D, et al. The study of trypanosome species circulating in domestic animals in two human African trypanosomiasis foci of Côte d'Ivoire identifies pigs and cattle as potential reservoirs of *Trypanosoma brucei gambiense*. *PLoS Negl Trop Dis*. 2017;11(10):e0005993. <https://doi.org/10.1371/journal.pntd.0005993> PMID: 29045405
8. Roger FL, Solano P, Bouyer J, Porphyre V, Berthier D, Peyre M, et al. Advocacy for identifying certain animal diseases as “neglected”. *PLoS Negl Trop Dis*. 2017;11(9):e0005843. <https://doi.org/10.1371/journal.pntd.0005843> PMID: 28880914
9. Antoine-Moussiaux N, Magez S, Desmacht D. Contributions of experimental mouse models to the understanding of African trypanosomiasis. *Trends Parasitol*. 2008;24(9):411–8. <https://doi.org/10.1016/j.pt.2008.05.010> PMID: 18684669
10. Magez S, Caljon G. Mouse models for pathogenic African trypanosomes: unravelling the immunology of host-parasite-vector interactions. *Parasite Immunol*. 2011;33(8):423–9. <https://doi.org/10.1111/j.1365-3024.2011.01293.x> PMID: 21480934
11. Moulton JE, Stevens DR. Animal model of human disease: trypanosomiasis, sleeping sickness. *Am J Pathol*. 1978;91(3):693–6. PMID: 655266
12. Kao WHL, Klag MJ, Meoni LA, Reich D, Berthier-Schaad Y, Li M, et al. MYH9 is associated with nondiabetic end-stage renal disease in African Americans. *Nat Genet*. 2008;40(10):1185–92. <https://doi.org/10.1038/ng.232> PMID: 18794854
13. Genovese G, Friedman DJ, Ross MD, Lecordier L, Uzureau P, Freedman BI, et al. Association of trypanolytic ApoL1 variants with kidney disease in African Americans. *Science*. 2010;329(5993):841–5. <https://doi.org/10.1126/science.1193032> PMID: 20647424
14. Berthier D, Brenière SF, Bras-Gonçalves R, Lemesre J-L, Jamonneau V, Solano P, et al. Tolerance to Trypanosomatids: A Threat, or a Key for Disease Elimination?. *Trends Parasitol*. 2016;32(2):157–68. <https://doi.org/10.1016/j.pt.2015.11.001> PMID: 26643519
15. Kemp SJ, Teale AJ. Genetic basis of trypanotolerance in cattle and mice. *Parasitol Today*. 1998;14(11):450–4. [https://doi.org/10.1016/s0169-4758\(98\)01334-9](https://doi.org/10.1016/s0169-4758(98)01334-9) PMID: 17040846
16. Truc P, Büscher P, Cuny G, Gonzatti MI, Jannin J, Joshi P, et al. Atypical human infections by animal trypanosomes. *PLoS Negl Trop Dis*. 2013;7(9):e2256. <https://doi.org/10.1371/journal.pntd.0002256> PMID: 24069464
17. Kumar R, Gupta S, Bhutia WD, Vaid RK, Kumar S. Atypical human trypanosomiasis: Potentially emerging disease with lack of understanding. *Zoonoses Public Health*. 2022;69(4):259–76. <https://doi.org/10.1111/zph.12945> PMID: 35355422
18. Okello I, Mafie E, Eastwood G, Nzalawahie J, Mboera LEG. African animal trypanosomiasis: a systematic review on prevalence, risk factors and drug resistance in sub-Saharan Africa. *J Med Entomol*. 2022;59(4):1099–143. <https://doi.org/10.1093/jme/tjac018> PMID: 35579072
19. Herrero M, Thornton PK. Livestock and global change: emerging issues for sustainable food systems. *Proc Natl Acad Sci U S A*. 2013;110(52):20878–81. <https://doi.org/10.1073/pnas.1321844111> PMID: 24344313
20. Thornton PK. Livestock production: recent trends, future prospects. *Philos Trans R Soc Lond B Biol Sci*. 2010;365(1554):2853–67. <https://doi.org/10.1098/rstb.2010.0134> PMID: 20713389
21. Hanotte O, Bradley DG, Ochieng JW, Verjee Y, Hill EW, Rege JEO. African pastoralism: genetic imprints of origins and migrations. *Science*. 2002;296(5566):336–9. <https://doi.org/10.1126/science.1069878> PMID: 11951043
22. MacHugh DE, Shriver MD, Loftus RT, Cunningham P, Bradley DG. Microsatellite DNA variation and the evolution, domestication and phylogeography of taurine and zebu cattle (*Bos taurus* and *Bos indicus*). *Genetics*. 1997;146(3):1071–86. <https://doi.org/10.1093/genetics/146.3.1071> PMID: 9215909
23. Kim J, Hanotte O, Mwai OA, Dessie T, Bashir S, Diallo B, et al. The genome landscape of indigenous African cattle. *Genome Biol*. 2017;18(1):34. <https://doi.org/10.1186/s13059-017-1153-y> PMID: 28219390

24. Mwai O, Hanotte O, Kwon Y-J, Cho S. African indigenous cattle: unique genetic resources in a rapidly changing world. *Asian-Australas J Anim Sci*. 2015;28(7):911–21. <https://doi.org/10.5713/ajas.15.0002R> PMID: 26104394
25. Holden CJ. Bantu language trees reflect the spread of farming across sub-Saharan Africa: a maximum-parsimony analysis. *Proc Biol Sci*. 2002;269(1493):793–9. <https://doi.org/10.1098/rspb.2002.1955> PMID: 11958710
26. Tishkoff SA, Reed FA, Friedlaender FR, Ehret C, Ranciaro A, Froment A, et al. The genetic structure and history of Africans and African Americans. *Science*. 2009;324(5930):1035–44. <https://doi.org/10.1126/science.1172257> PMID: 19407144
27. Yaro M, Munyard KA, Stear MJ, Groth DM. Combatting African Animal Trypanosomiasis (AAT) in livestock: The potential role of trypanotolerance. *Vet Parasitol*. 2016;225:43–52. <https://doi.org/10.1016/j.vetpar.2016.05.003> PMID: 27369574
28. Freeman AR, Meghen CM, MacHugh DE, Loftus RT, Achukwi MD, Bado A, et al. Admixture and diversity in West African cattle populations. *Mol Ecol*. 2004;13(11):3477–87. <https://doi.org/10.1111/j.1365-294X.2004.02311.x> PMID: 15488005
29. Murray M, Trail JC, D'Ieteren GD. Trypanotolerance in cattle and prospects for the control of trypanosomiasis by selective breeding. *Rev Sci Tech*. 1990;9(2):369–86. <https://doi.org/10.20506/rst.9.2.506> PMID: 2132686
30. Murray M, Black SJ. African trypanosomiasis in cattle: working with nature's solution. *Vet Parasitol*. 1985;18(2):167–82. [https://doi.org/10.1016/0304-4017\(85\)90065-2](https://doi.org/10.1016/0304-4017(85)90065-2) PMID: 3898544
31. d'Ieteren GD, Authié E, Wissocq N, Murray M. Trypanotolerance, an option for sustainable livestock production in areas at risk from trypanosomiasis. *Rev Sci Tech*. 1998;17(1):154–75. <https://doi.org/10.20506/rst.17.1.1088> PMID: 9638808
32. Trail JC, D'Ieteren GD, Teale AJ. Trypanotolerance and the value of conserving livestock genetic resources. *Genome*. 1989;31(2):805–12. <https://doi.org/10.1139/g89-142> PMID: 2534387
33. Smetko A, Soudre A, Silbermayr K, Müller S, Brem G, Hanotte O, et al. Trypanosomosis: potential driver of selection in African cattle. *Front Genet*. 2015;6:137. <https://doi.org/10.3389/fgene.2015.00137> PMID: 25964796
34. Noyes H, Brass A, Obara I, Anderson S, Archibald AL, Bradley DG, et al. Genetic and expression analysis of cattle identifies candidate genes in pathways responding to *Trypanosoma congolense* infection. *Proc Natl Acad Sci U S A*. 2011;108(22):9304–9. <https://doi.org/10.1073/pnas.1013486108> PMID: 21593421
35. Naessens J, Teale AJ, Sileghem M. Identification of mechanisms of natural resistance to African trypanosomiasis in cattle. *Vet Immunol Immunopathol*. 2002;87(3–4):187–94. [https://doi.org/10.1016/s0165-2427\(02\)00070-3](https://doi.org/10.1016/s0165-2427(02)00070-3) PMID: 12072233
36. Trail JC, d'Ieteren GD, Maille JC, Yangari G. Genetic aspects of control of anaemia development in trypanotolerant N'Dama cattle. *Acta Trop*. 1991;48(4):285–91. [https://doi.org/10.1016/0001-706x\(91\)90016-d](https://doi.org/10.1016/0001-706x(91)90016-d) PMID: 1674402
37. Gautier M, Flori L, Riebler A, Jaffrézic F, Laloé D, Gut I, et al. A whole genome Bayesian scan for adaptive genetic divergence in West African cattle. *BMC Genomics*. 2009;10:550. <https://doi.org/10.1186/1471-2164-10-550> PMID: 19930592
38. Kim S-J, Ka S, Ha J-W, Kim J, Yoo D, Kim K, et al. Cattle genome-wide analysis reveals genetic signatures in trypanotolerant N'Dama. *BMC Genomics*. 2017;18(1):371. <https://doi.org/10.1186/s12864-017-3742-2> PMID: 28499406
39. Hill EW, O'Gorman GM, Agaba M, Gibson JP, Hanotte O, Kemp SJ, et al. Understanding bovine trypanosomiasis and trypanotolerance: the promise of functional genomics. *Vet Immunol Immunopathol*. 2005;105(3–4):247–58. <https://doi.org/10.1016/j.vetimm.2005.02.004> PMID: 15808304
40. Meade KG, O'Gorman GM, Hill EW, Narciandi F, Agaba M, Kemp SJ, et al. Divergent antimicrobial peptide (AMP) and acute phase protein (APP) responses to *Trypanosoma congolense* infection in trypanotolerant and trypanosusceptible cattle. *Mol Immunol*. 2009;47(2–3):196–204. <https://doi.org/10.1016/j.molimm.2009.09.042> PMID: 19889461
41. O'Gorman GM, Park SDE, Hill EW, Meade KG, Coussens PM, Agaba M, et al. Transcriptional profiling of cattle infected with *Trypanosoma congolense* highlights gene expression signatures underlying trypanotolerance and trypanosusceptibility. *BMC Genomics*. 2009;10:207. <https://doi.org/10.1186/1471-2164-10-207> PMID: 19409086
42. O'Gorman GM, Park SDE, Hill EW, Meade KG, Mitchell LC, Agaba M, et al. Cytokine mRNA profiling of peripheral blood mononuclear cells from trypanotolerant and trypanosusceptible cattle infected with *Trypanosoma congolense*. *Physiol Genomics*. 2006;28(1):53–61. <https://doi.org/10.1152/physiolgenomics.00100.2006> PMID: 16985010
43. Peylhard M, Berthier D, Dayo G-K, Chantal I, Sylla S, Nidelet S, et al. Whole blood transcriptome profiles of trypanotolerant and trypanosusceptible cattle highlight a differential modulation of metabolism and immune response during infection by *Trypanosoma congolense*. *Peer Community Journal*. 2023;3. <https://doi.org/10.24072/pcjournal.239>
44. Dayo GK, Gautier M, Berthier D, Poivey JP, Sidibe I, Bengaly Z, et al. Association studies in QTL regions linked to bovine trypanotolerance in a West African crossbred population. *Anim Genet*. 2012;43(2):123–32. <https://doi.org/10.1111/j.1365-2052.2011.02227.x> PMID: 22404348
45. Bahbhaní H, Afana A, Wragg D. Genomic signatures of adaptive introgression and environmental adaptation in the Sheko cattle of southwest Ethiopia. *PLoS One*. 2018;13(8):e0202479. <https://doi.org/10.1371/journal.pone.0202479> PMID: 30114214
46. Berthier D, Peylhard M, Dayo G-K, Flori L, Sylla S, Bolly S, et al. A comparison of phenotypic traits related to trypanotolerance in five West African cattle breeds highlights the value of shorthorn taurine breeds. *PLoS One*. 2015;10(5):e0126498. <https://doi.org/10.1371/journal.pone.0126498> PMID: 25954819
47. Álvarez I, Pérez-Pardal L, Traoré A, Fernández I, Goyache F. Lack of haplotype structuring for two candidate genes for trypanotolerance in cattle. *J Anim Breed Genet*. 2016;133(2):105–14. <https://doi.org/10.1111/jbg.12181> PMID: 26365013

48. Goyache F, Pérez-Pardal L, Fernández I, Traoré A, Menéndez-Arias NA, Álvarez I. Ancient autozygous segments subject to positive selection suggest adaptive immune responses in West African cattle. *Gene*. 2021;803:145899. <https://doi.org/10.1016/j.gene.2021.145899> PMID: 34400278
49. Rajavel A, Heinrich F, Schmitt AO, Gültas M. Identifying cattle breed-specific partner choice of transcription factors during the African trypanosomiasis disease progression using bioinformatics analysis. *Vaccines (Basel)*. 2020;8(2):246. <https://doi.org/10.3390/vaccines8020246> PMID: 32456126
50. Rajavel A, Klees S, Hui Y, Schmitt AO, Gültas M. Deciphering the molecular mechanism underlying African animal trypanosomiasis by means of the 1000 bull genomes project genomic dataset. *Biology (Basel)*. 2022;11(5):742. <https://doi.org/10.3390/biology11050742> PMID: 35625470
51. Geigy R, Kauffmann M. Sleeping sickness survey in the Serengeti area (Tanzania) 1971. I. Examination of large mammals for trypanosomes. *Acta Trop*. 1973;30(1):12–23. PMID: 4144952
52. Nantulya VM, Musoke AJ, Rurangirwa FR, Moloo SK. Resistance of cattle to tsetse-transmitted challenge with *Trypanosoma brucei* or *Trypanosoma congolense* after spontaneous recovery from syringe-passaged infections. *Infect Immun*. 1984;43(2):735–8. <https://doi.org/10.1128/iai.43.2.735-738.1984> PMID: 6693173
53. Akol GW, Murray M. Early events following challenge of cattle with tsetse infected with *Trypanosoma congolense*: development of the local skin reaction. *Vet Rec*. 1982;110(13):295–302. <https://doi.org/10.1136/vr.110.13.295> PMID: 7072104
54. Dwinger RH, Murray M, Moloo SK. Potential value of localized skin reactions (chancres) induced by *Trypanosoma congolense* transmitted by *Glossina morsitans centralis* for the analysis of metacyclic trypanosome populations. *Parasite Immunol*. 1987;9(3):353–62. <https://doi.org/10.1111/j.1365-3024.1987.tb00513.x> PMID: 3601446
55. Frerebeau N. Khroma: Colour Schemes for Scientific Data Visualization. manual. Report No. 2023.
56. Garnier S, Ross N, Rudis R. Viridis (Lite) - Colorblind-Friendly Color Maps for R. manual. 2023.
57. Gautier L, Cope L, Bolstad BM, Irizarry RA. affy--analysis of Affymetrix GeneChip data at the probe level. *Bioinformatics*. 2004;20(3):307–15. <https://doi.org/10.1093/bioinformatics/btg405> PMID: 14960456
58. Huber W, Carey VJ, Gentleman R, Anders S, Carlson M, Carvalho BS, et al. Orchestrating high-throughput genomic analysis with Bioconductor. *Nat Methods*. 2015;12(2):115–21. <https://doi.org/10.1038/nmeth.3252> PMID: 25633503
59. Kauffmann A, Gentleman R, Huber W. Arrayqualitymetrics--a bioconductor package for quality assessment of microarray data. *Bioinformatics*. 2009;25(3):415–6. <https://doi.org/10.1093/bioinformatics/btn647> PMID: 19106121
60. R Core Team. R: A Language and Environment for Statistical Computing. Vienna, Austria: R Foundation for Statistical Computing. 2023.
61. Rue-Albrecht K, Magee DA, Killick KE, Nalpas NC, Gordon SV, MacHugh DE. Comparative functional genomics and the bovine macrophage response to strains of the mycobacterium genus. *Front Immunol*. 2014;5:536. <https://doi.org/10.3389/fimmu.2014.00536> PMID: 25414700
62. Hochreiter S, Clevert D-A, Obermayer K. A new summarization method for Affymetrix probe level data. *Bioinformatics*. 2006;22(8):943–9. <https://doi.org/10.1093/bioinformatics/bt033> PMID: 16473874
63. Wickham H, François R, Henry L, Müller K, Vaughan D. dplyr: A Grammar of Data Manipulation. 2023. Report No.
64. van den Brand T. Ggh4x: Hacks for 'ggplot2'. 2023.
65. Wickham H. ggplot2: Elegant Graphics for Data Analysis. New York: Springer. 2009.
66. Wilke CO, Wiernik BM. ggttext: Improved Text Rendering Support for 'ggplot2'. 2022.
67. Bache SM, Wickham H. Magrittr: A Forward-Pipe Operator for R. 2022.
68. Wickham H, Hester J, Bryan J. Readr: Read Rectangular Text Data. 2023.
69. Wickham H. Reshaping Data with thereshapePackage. *J Stat Soft*. 2007;21(12). <https://doi.org/10.18637/jss.v021.i12>
70. Wickham H. Stringr: Simple, Consistent Wrappers for Common String Operations. 2023.
71. Ritchie ME, Phipson B, Wu D, Hu Y, Law CW, Shi W, et al. limma powers differential expression analyses for RNA-sequencing and microarray studies. *Nucleic Acids Res*. 2015;43(7):e47. <https://doi.org/10.1093/nar/gkv007> PMID: 25605792
72. Pedersen TL. Patchwork: The Composer of Plots. 2023.
73. Smyth GK, Michaud J, Scott HS. Use of within-array replicate spots for assessing differential expression in microarray experiments. *Bioinformatics*. 2005;21(9):2067–75. <https://doi.org/10.1093/bioinformatics/bti270> PMID: 15657102
74. Smyth GK. Linear models and empirical bayes methods for assessing differential expression in microarray experiments. *Stat Appl Genet Mol Biol*. 2004;3:Article3. <https://doi.org/10.2202/1544-6115.1027> PMID: 16646809
75. Benjamini Y, Hochberg Y. Controlling the false discovery rate: a practical and powerful approach to multiple testing. *J Roy Stat Soc B Met*. 1995;57(1):289–300.
76. Kolberg L, Raudvere U, Kuzmin I, Adler P, Vilo J, Peterson H. g:Profiler-interoperable web service for functional enrichment analysis and gene identifier mapping (2023 update). *Nucleic Acids Res*. 2023;51(W1):W207–12. <https://doi.org/10.1093/nar/gkad347> PMID: 37144459
77. Krassowski M. ComplexUpset. 2020.
78. Slowikowski K. Ggrepel: Automatically position non-overlapping text labels with 'ggplot2'. 2023. Report No.
79. Henry L, Wickham H. rlang: Functions for Base Types and Core R and 'tidyverse' Features. 2024. Report No.
80. Wickham H, Vaughan D, Girlich M. Tidyr: Tidy Messy Data. 2023.

81. Ooms J. Magick: Advanced Graphics and Image-Processing in R. 2023. Report No.
82. ImageMagick Studio LLC. ImageMagick. 2023.
83. Wickham H, Henry L. Purrr: Functional Programming Tools. 2023. Report No.
84. Wickham H, Pedersen TL, Seidel D. Scales: Scale Functions for Visualization. manual. 2023. Report No.
85. Merico D, Isserlin R, Stueker O, Emili A, Bader GD. Enrichment map: a network-based method for gene-set enrichment visualization and interpretation. *PLoS One*. 2010;5(11):e13984. <https://doi.org/10.1371/journal.pone.0013984> PMID: 21085593
86. Shannon P, Markiel A, Ozier O, Baliga NS, Wang JT, Ramage D, et al. Cytoscape: a software environment for integrated models of biomolecular interaction networks. *Genome Res*. 2003;13(11):2498–504. <https://doi.org/10.1101/gr.1239303> PMID: 14597658
87. Reimand J, Isserlin R, Voisin V, Kucera M, Tannus-Lopes C, Rostamianfar A, et al. Pathway enrichment analysis and visualization of omics data using g:Profiler, GSEA, Cytoscape and EnrichmentMap. *Nat Protoc*. 2019;14(2):482–517. <https://doi.org/10.1038/s41596-018-0103-9> PMID: 30664679
88. Kucera M, Isserlin R, Arkhangorodsky A, Bader GD. AutoAnnotate: A Cytoscape app for summarizing networks with semantic annotations. *F1000Res*. 2016;5:1717. <https://doi.org/10.12688/f1000research.9090.1> PMID: 27830058
89. Morris JH, Apeltsin L, Newman AM, Baumbach J, Wittkop T, Su G, et al. clusterMaker: a multi-algorithm clustering plugin for Cytoscape. *BMC Bioinformatics*. 2011;12:436. <https://doi.org/10.1186/1471-2105-12-436> PMID: 22070249
90. Oesper L, Merico D, Isserlin R, Bader GD. WordCloud: a Cytoscape plugin to create a visual semantic summary of networks. *Source Code Biol Med*. 2011;6:7. <https://doi.org/10.1186/1751-0473-6-7> PMID: 21473782
91. Becker MY, Rojas I. A graph layout algorithm for drawing metabolic pathways. *Bioinformatics*. 2001;17(5):461–7. <https://doi.org/10.1093/bioinformatics/17.5.461> PMID: 11331241
92. Magee DA, Taraktsoglou M, Killick KE, Nalpas NC, Browne JA, Park SDE, et al. Global gene expression and systems biology analysis of bovine monocyte-derived macrophages in response to in vitro challenge with *Mycobacterium bovis*. *PLoS One*. 2012;7(2):e32034. <https://doi.org/10.1371/journal.pone.0032034> PMID: 22384131
93. Machugh DE, Taraktsoglou M, Killick KE, Nalpas NC, Browne JA, DE Park S, et al. Pan-genomic analysis of bovine monocyte-derived macrophage gene expression in response to in vitro infection with *Mycobacterium avium* subspecies paratuberculosis. *Vet Res*. 2012;43(1):25. <https://doi.org/10.1186/1297-9716-43-25> PMID: 22455317
94. Killick KE, Browne JA, Park SDE, Magee DA, Martin I, Meade KG, et al. Genome-wide transcriptional profiling of peripheral blood leukocytes from cattle infected with *Mycobacterium bovis* reveals suppression of host immune genes. *BMC Genomics*. 2011;12:611. <https://doi.org/10.1186/1471-2164-12-611> PMID: 22182502
95. Ezendam J, Staedtler F, Pennings J, Vandebril RJ, Pieters R, Harleman JH, et al. Toxicogenomics of subchronic hexachlorobenzene exposure in Brown Norway rats. *Environ Health Perspect*. 2004;112(7):782–91. <https://doi.org/10.1289/ehp.112-1241993> PMID: 15159207
96. Kriegel HP, Kröger P, Schubert E, Zimek A. A general framework for increasing the robustness of PCA-based correlation clustering algorithms. Berlin, Heidelberg: Springer Berlin Heidelberg. 2008.
97. McVean G. A genealogical interpretation of principal components analysis. *PLoS Genet*. 2009;5(10):e1000686. <https://doi.org/10.1371/journal.pgen.1000686> PMID: 19834557
98. Novembre J, Stephens M. Interpreting principal component analyses of spatial population genetic variation. *Nat Genet*. 2008;40(5):646–9. <https://doi.org/10.1038/ng.139> PMID: 18425127
99. Lewis SM, Williams A, Eisenbarth SC. Structure and function of the immune system in the spleen. *Sci Immunol*. 2019;4(33):eaau6085. <https://doi.org/10.1126/sciimmunol.aau6085> PMID: 30824527
100. Buettner M, Bode U. Lymph node dissection—understanding the immunological function of lymph nodes. *Clin Exp Immunol*. 2012;169(3):205–12. <https://doi.org/10.1111/j.1365-2249.2012.04602.x> PMID: 22861359
101. Jönsson V. Comparison and definition of spleen and lymph node: a phylogenetic analysis. *J Theor Biol*. 1985;117(4):691–9. [https://doi.org/10.1016/s0022-5193\(85\)80247-2](https://doi.org/10.1016/s0022-5193(85)80247-2) PMID: 4094460
102. Dalma-Weiszhausz DD, Warrington J, Tanimoto EY, Miyada CG. The affymetrix GeneChip platform: an overview. *Methods Enzymol*. 2006;410:3–28. [https://doi.org/10.1016/S0076-6879\(06\)10001-4](https://doi.org/10.1016/S0076-6879(06)10001-4) PMID: 16938544
103. Casey ME, Meade KG, Nalpas NC, Taraktsoglou M, Browne JA, Killick KE, et al. Analysis of the Bovine Monocyte-Derived Macrophage Response to *Mycobacterium avium* Subspecies Paratuberculosis Infection Using RNA-seq. *Front Immunol*. 2015;6:23. <https://doi.org/10.3389/fimmu.2015.00023> PMID: 25699042
104. McLoughlin KE, Nalpas NC, Rue-Albrecht K, Browne JA, Magee DA, Killick KE, et al. RNA-seq Transcriptional Profiling of Peripheral Blood Leukocytes from Cattle Infected with *Mycobacterium bovis*. *Front Immunol*. 2014;5:396. <https://doi.org/10.3389/fimmu.2014.00396> PMID: 25206354
105. Nalpas NC, Park SDE, Magee DA, Taraktsoglou M, Browne JA, Conlon KM, et al. Whole-transcriptome, high-throughput RNA sequence analysis of the bovine macrophage response to *Mycobacterium bovis* infection in vitro. *BMC Genomics*. 2013;14:230. <https://doi.org/10.1186/1471-2164-14-230> PMID: 23565803
106. Gitau JK, Macharia RW, Mwangi KW, Ongeso N, Murungi E. Gene co-expression network identifies critical genes, pathways and regulatory motifs mediating the progression of rift valley fever in *Bos taurus*. *Heliyon*. 2023;9(7):e18175. <https://doi.org/10.1016/j.heliyon.2023.e18175> PMID: 37519716

107. Kuiper JWP, Krause J, Potgeter L, Adrian J, Hauck CR. A genome-wide genetic screen identifies CYRI-B as a negative regulator of CEACAM3-mediated phagocytosis. *J Cell Sci.* 2023;136(11):jcs260771. <https://doi.org/10.1242/jcs.260771> PMID: 37264948
108. Al Barashdi MA, Ali A, McMullin MF, Mills K. Protein tyrosine phosphatase receptor type C (PTPRC or CD45). *J Clin Pathol.* 2021;74(9):548–52. <https://doi.org/10.1136/jclinpath-2020-206927> PMID: 34039664
109. Goodhead I, Archibald A, Amwayi P, Brass A, Gibson J, Hall N, et al. A comprehensive genetic analysis of candidate genes regulating response to *Trypanosoma congolense* infection in mice. *PLoS Negl Trop Dis.* 2010;4(11):e880. <https://doi.org/10.1371/journal.pntd.0000880> PMID: 21085469
110. Noyes HA, Alimohammadian MH, Agaba M, Brass A, Fuchs H, Gailus-Durner V, et al. Mechanisms controlling anaemia in *Trypanosoma congolense* infected mice. *PLoS One.* 2009;4(4):e5170. <https://doi.org/10.1371/journal.pone.0005170> PMID: 19365556
111. Guerrero NA, Camacho M, Vila L, Íñiguez MA, Chillón-Marinas C, Cuervo H, et al. Cyclooxygenase-2 and Prostaglandin E2 Signaling through Prostaglandin Receptor EP-2 Favor the Development of Myocarditis during Acute *Trypanosoma cruzi* Infection. *PLoS Negl Trop Dis.* 2015;9(8):e0004025. <https://doi.org/10.1371/journal.pntd.0004025> PMID: 26305786
112. Pham HTT, Magez S, Choi B, Baatar B, Jung J, Radwanska M. Neutrophil metalloproteinase driven spleen damage hampers infection control of trypanosomiasis. *Nat Commun.* 2023;14(1):5418. <https://doi.org/10.1038/s41467-023-41089-w> PMID: 37669943
113. Antoine-Moussiaux N, Cornet A, Cornet F, Glineur S, Dermine M, Desmecht D. A non-cytosolic protein of *Trypanosoma evansi* induces CD45-dependent lymphocyte death. *PLoS One.* 2009;4(5):e5728. <https://doi.org/10.1371/journal.pone.0005728> PMID: 19478957
114. Le Coz C, Nguyen DN, Su C, Nolan BE, Albrecht AV, Xhani S, et al. Constrained chromatin accessibility in PU.1-mutated agammaglobulinemia patients. *J Exp Med.* 2021;218(7):e20201750. <https://doi.org/10.1084/jem.20201750> PMID: 33951726
115. Liu W, Rodgers GP. Olfactomedin 4 expression and functions in innate immunity, inflammation, and cancer. *Cancer Metastasis Rev.* 2016;35(2):201–12. <https://doi.org/10.1007/s10555-016-9624-2> PMID: 27178440
116. Tanioku T, Nishibata M, Tokinaga Y, Konno K, Watanabe M, Hemmi H, et al. Tmem45b is essential for inflammation- and tissue injury-induced mechanical pain hypersensitivity. *Proc Natl Acad Sci U S A.* 2022;119(45):e2121989119. <https://doi.org/10.1073/pnas.2121989119> PMID: 36322717
117. Röder A, Hüskens S, Hutter MC, Rettie AE, Hanenberg H, Wiek C, et al. Spotlight on CYP4B1. *Int J Mol Sci.* 2023;24(3):2038. <https://doi.org/10.3390/ijms24032038> PMID: 36768362
118. Banworth MJ, Liang Z, Li G. A novel membrane targeting domain mediates the endosomal or Golgi localization specificity of small GTPases Rab22 and Rab31. *J Biol Chem.* 2022;298(9):102281. <https://doi.org/10.1016/j.jbc.2022.102281> PMID: 35863437
119. Jentsch J, Wunderlich H, Thein M, Bechthold J, Brehm L, Krauss SW, et al. Microtubule polyglutamylation is an essential regulator of cytoskeletal integrity in *Trypanosoma brucei*. *J Cell Sci.* 2024;137(3):jcs261740. <https://doi.org/10.1242/jcs.261740> PMID: 38205672
120. Kumar R, Ali SA, Singh SK, Bhushan V, Mathur M, Jamwal S, et al. Antimicrobial Peptides in Farm Animals: An Updated Review on Its Diversity, Function, Modes of Action and Therapeutic Prospects. *Vet Sci.* 2020;7(4):206. <https://doi.org/10.3390/vetsci7040206> PMID: 33352919
121. Davies D, Meade KG, Herath S, Eckersall PD, Gonzalez D, White JO, et al. Toll-like receptor and antimicrobial peptide expression in the bovine endometrium. *Reprod Biol Endocrinol.* 2008;6:53. <https://doi.org/10.1186/1477-7827-6-53> PMID: 19017375
122. Tetens J, Friedrich JJ, Hartmann A, Schwerin M, Kalm E, Thaller G. The spatial expression pattern of antimicrobial peptides across the healthy bovine udder. *J Dairy Sci.* 2010;93(2):775–83. <https://doi.org/10.3168/jds.2009-2729> PMID: 20105549
123. Alva-Murillo N, Téllez-Pérez AD, Sagrero-Cisneros E, López-Meza JE, Ochoa-Zarzosa A. Expression of antimicrobial peptides by bovine endothelial cells. *Cell Immunol.* 2012;280(1):108–12. <https://doi.org/10.1016/j.cellimm.2012.11.016> PMID: 23298865
124. Krause A, Sillard R, Kleemeier B, Klüver E, Maronde E, Conejo-García JR, et al. Isolation and biochemical characterization of LEAP-2, a novel blood peptide expressed in the liver. *Protein Sci.* 2003;12(1):143–52. <https://doi.org/10.1101/ps.0213603> PMID: 12493837
125. Whelehan CJ, Barry-Reidy A, Meade KG, Eckersall PD, Chapwanya A, Narciandi F, et al. Characterisation and expression profile of the bovine cathelicidin gene repertoire in mammary tissue. *BMC Genomics.* 2014;15:128. <https://doi.org/10.1186/1471-2164-15-128> PMID: 24524771
126. McGwire BS, Olson CL, Tack BF, Engman DM. Killing of African trypanosomes by antimicrobial peptides. *J Infect Dis.* 2003;188(1):146–52. <https://doi.org/10.1086/375747> PMID: 12825184
127. Selsted ME, Tang YQ, Morris WL, McGuire PA, Novotny MJ, Smith W, et al. Purification, primary structures, and antibacterial activities of beta-defensins, a new family of antimicrobial peptides from bovine neutrophils. *J Biol Chem.* 1993;268(9):6641–8. PMID: 8454635
128. Regenhard P, Leippe M, Schubert S, Podschun R, Kalm E, Grötzinger J, et al. Antimicrobial activity of bovine psoriasin. *Vet Microbiol.* 2009;136(3–4):335–40. <https://doi.org/10.1016/j.vetmic.2008.12.001> PMID: 19167844
129. Uzonna JE, Kaushik RS, Gordon JR, Tabel H. Cytokines and antibody responses during *Trypanosoma congolense* infections in two inbred mouse strains that differ in resistance. *Parasite Immunol.* 1999;21(2):57–71. <https://doi.org/10.1046/j.1365-3024.1999.00202.x> PMID: 10101716
130. Quintana JF, Sinton MC, Chandrasegaran P, Kumar Dubey L, Ogunsola J, Al Samman M, et al. The murine meninges acquire lymphoid tissue properties and harbour autoreactive B cells during chronic *Trypanosoma brucei* infection. *PLoS Biol.* 2023;21(11):e3002389. <https://doi.org/10.1371/journal.pbio.3002389> PMID: 37983289
131. Choi B, Vu HT, Vu HT, Radwanska M, Magez S. Advances in the Immunology of the Host-Parasite Interactions in African Trypanosomosis, including Single-Cell Transcriptomics. *Pathogens.* 2024;13(3):188. <https://doi.org/10.3390/pathogens13030188> PMID: 38535532
132. Rivera-Correa J, Verdi J, Sherman J, Sternberg JM, Raper J, Rodriguez A. Autoimmunity to phosphatidylserine and anemia in African Trypanosome infections. *PLoS Negl Trop Dis.* 2021;15(9):e0009814. <https://doi.org/10.1371/journal.pntd.0009814> PMID: 34587165

133. Soares-Silva M, Diniz FF, Gomes GN, Bahia D. The Mitogen-Activated Protein Kinase (MAPK) Pathway: Role in Immune Evasion by Trypanosomatids. *Front Microbiol.* 2016;7:183. <https://doi.org/10.3389/fmicb.2016.00183> PMID: 26941717
134. Kaur P, Goyal N. Pathogenic role of mitogen activated protein kinases in protozoan parasites. *Biochimie.* 2022;193:78–89. <https://doi.org/10.1016/j.biochi.2021.10.012> PMID: 34706251
135. Kuriakose S, Onyilagha C, Singh R, Olayinka-Adefemi F, Jia P, Uzonna JE. TLR-2 and MyD88-Dependent Activation of MAPK and STAT Proteins Regulates Proinflammatory Cytokine Response and Immunity to Experimental *Trypanosoma congolense* Infection. *Front Immunol.* 2019;10:2673. <https://doi.org/10.3389/fimmu.2019.02673> PMID: 31824484
136. Pays E, Vanhollebeke B, Vanhamme L, Paturiaux-Hanocq F, Nolan DP, Pérez-Morga D. The trypanolytic factor of human serum. *Nat Rev Microbiol.* 2006;4(6):477–86. <https://doi.org/10.1038/nrmicro1428> PMID: 16710327
137. Welde BT, Chumo DA, Onyango FK, Reardon MJ, Roberts LM, Njogu AR, et al. Trypanosoma vivax: disseminated intravascular coagulation in cattle. *Ann Trop Med Parasitol.* 1989;83 Suppl 1:177–83. <https://doi.org/10.1080/00034983.1989.11812422> PMID: 2619392
138. Greenwood BM, Whittle HC. Coagulation studies in Gambian trypanosomiasis. *Am J Trop Med Hyg.* 1976;25(3):390–4. <https://doi.org/10.4269/ajtmh.1976.25.390> PMID: 937630
139. Choudhuri S, Garg NJ. Platelets, Macrophages, and Thromboinflammation in Chagas Disease. *J Inflamm Res.* 2022;15:5689–706. <https://doi.org/10.2147/JIR.S380896> PMID: 36217453
140. Naessens J. Bovine trypanotolerance: A natural ability to prevent severe anaemia and haemophagocytic syndrome?. *Int J Parasitol.* 2006;36(5):521–8. <https://doi.org/10.1016/j.ijpara.2006.02.012> PMID: 16678182
141. Stijlemans B, Beschin A, Magez S, Van Ginderachter JA, De Baetselier P. Iron Homeostasis and *Trypanosoma brucei* Associated Immunopathogenicity Development: A Battle/Quest for Iron. *Biomed Res Int.* 2015;2015:819389. <https://doi.org/10.1155/2015/819389> PMID: 26090446
142. Magez S, Schwegmann A, Atkinson R, Claes F, Drennan M, De Baetselier P, et al. The role of B-cells and IgM antibodies in parasitemia, anemia, and VSG switching in *Trypanosoma brucei*-infected mice. *PLoS Pathog.* 2008;4(8):e1000122. <https://doi.org/10.1371/journal.ppat.1000122> PMID: 18688274
143. Gilabert Carbajo C, Cornell LJ, Madbouly Y, Lai Z, Yates PA, Tinti M, et al. Novel aspects of iron homeostasis in pathogenic bloodstream form *Trypanosoma brucei*. *PLoS Pathog.* 2021;17(6):e1009696. <https://doi.org/10.1371/journal.ppat.1009696> PMID: 34161395
144. Taylor MC, Kelly JM. Iron metabolism in trypanosomatids, and its crucial role in infection. *Parasitology.* 2010;137(6):899–917. <https://doi.org/10.1017/S0031182009991880> PMID: 20152063
145. Dick CF, Alcantara CL, Carvalho-Kelly LF, Lacerda-Abreu MA, Cunha-E-Silva NL, Meyer-Fernandes JR, et al. Iron Uptake Controls *Trypanosoma cruzi* Metabolic Shift and Cell Proliferation. *Antioxidants (Basel).* 2023;12(5):984. <https://doi.org/10.3390/antiox12050984> PMID: 37237850
146. Basu S, Horáková E, Lukeš J. Iron-associated biology of *Trypanosoma brucei*. *Biochim Biophys Acta.* 2016;1860(2):363–70. <https://doi.org/10.1016/j.bbagen.2015.10.027> PMID: 26523873
147. Steverding D. Bloodstream forms of *Trypanosoma brucei* require only small amounts of iron for growth. *Parasitol Res.* 1998;84(1):59–62. <https://doi.org/10.1007/s004360050357> PMID: 9491428
148. Stijlemans B, Vankrunkelsven A, Brys L, Magez S, De Baetselier P. Role of iron homeostasis in trypanosomiasis-associated anemia. *Immunobiology.* 2008;213(9–10):823–35. <https://doi.org/10.1016/j.imbio.2008.07.023> PMID: 18926297
149. Stijlemans B, Vankrunkelsven A, Caljon G, Bockstal V, Guilliams M, Bosschaerts T, et al. The central role of macrophages in trypanosomiasis-associated anemia: rationale for therapeutic approaches. *Endocr Metab Immune Disord Drug Targets.* 2010;10(1):71–82. <https://doi.org/10.2174/187153010790827966> PMID: 20158497
150. Naessens J, Leak SGA, Kennedy DJ, Kemp SJ, Teale AJ. Responses of bovine chimaeras combining trypanosomosis resistant and susceptible genotypes to experimental infection with *Trypanosoma congolense*. *Vet Parasitol.* 2003;111(2–3):125–42. [https://doi.org/10.1016/s0304-4017\(02\)00360-6](https://doi.org/10.1016/s0304-4017(02)00360-6) PMID: 12531289
151. Donovan A, Lima CA, Pinkus JL, Pinkus GS, Zon LI, Robine S, et al. The iron exporter ferroportin/Slc40a1 is essential for iron homeostasis. *Cell Metab.* 2005;1(3):191–200. <https://doi.org/10.1016/j.cmet.2005.01.003> PMID: 16054062
152. Holder A, Garty R, Elder C, Mesnard P, Laquerbe C, Bartens M-C, et al. Analysis of Genetic Variation in the Bovine SLC11A1 Gene, Its Influence on the Expression of NRAMP1 and Potential Association With Resistance to Bovine Tuberculosis. *Front Microbiol.* 2020;11:1420. <https://doi.org/10.3389/fmicb.2020.01420> PMID: 32714308
153. Archer NS, Nassif NT, O'Brien BA. Genetic variants of SLC11A1 are associated with both autoimmune and infectious diseases: systematic review and meta-analysis. *Genes Immun.* 2015;16(4):275–83. <https://doi.org/10.1038/gene.2015.8> PMID: 25856512